Barriers to the Transport of Diffusive Scalars in Compressible Flows[*]

George Haller[†], Daniel Karrasch[‡], and Florian Kogelbauer[†]

Abstract. Our recent work identifies material surfaces in incompressible flows that extremize the transport of an arbitrary, weakly diffusive scalar field relative to neighboring surfaces. Such barriers and enhancers of transport can be located directly from the deterministic component of the velocity field without diffusive or stochastic simulations. Here we extend these results to compressible flows and to diffusive concentration fields affected by sources or sinks, as well as by spontaneous decay. We construct diffusive transport extremizers with and without constraining them on a specific initial concentration distribution. For two-dimensional flows, we obtain explicit differential equations and a diagnostic scalar field that identify the most observable extremizers with pointwise uniform transport density. We illustrate our results by uncovering diffusion barriers and enhancers in analytic, numerical, and observational velocity fields.

Key words. transport barriers, invariant manifolds, stochastic transport, diffusive transport, coherent structures

AMS subject classifications. 76-xx, 37-xx, 49-xx

DOI. 10.1137/19M1238666

1. Introduction. Transport barriers can informally be defined as observed inhibitors of the spread of substances in a flow. They are well documented in geophysics [36], classical fluid dynamics [26], plasma fusion [8], reactive flows [30], and molecular dynamics [35], yet no general theory for them has been available until recently. In [15], we have put forward such a theory for incompressible flows and weakly diffusing substances by defining and solving an extremum problem for material surfaces that block the diffusive transport of passive scalars more than neighboring surfaces do.

The a priori restriction of this optimization problem to material surfaces (codimension-one invariant manifolds of the flow in the extended phase space of positions and time) is justified by the complete lack of advective transport across such invariant surfaces. Indeed, for small enough diffusivities, pointwise, finite-time, advective transport through any nonmaterial

[†]Corresponding author. Institute for Mechanical Systems, ETH Zürich, 8092 Zürich, Switzerland (georgehaller@ethz.ch, kogelbauer@mavt.ethz.ch).
[‡]Zentrum Mathematik–M3, Technische Universität München, 85748 Garching, Germany (karrasch@ma.tum.de).

(i.e., noninvariant) surface is always larger than diffusive transport. As a consequence, in the range of small diffusivities, one should seek transport barriers among material surfaces.

Such barriers turn out to be computable and depend on the structure of the diffusion tensor but not on the actual value of the diffusivities [15]. Thus, diffusion barriers remain well defined in the limit of nondiffusive, purely advective transport. In that limit, they form surfaces that will prevail as transport inhibitors or enhancers under the presence of the slightest diffusion or uncertainty modeled by Brownian motion. This gives a transport-barrier definition in the advective limit, independent of any preferred coherence principle and based solely on the physically well-defined and quantitative notion of diffusive transport through a surface. This limiting property of diffusion barriers eliminates the current ambiguity in locating coherent structures in finite-time, advective transport where different coherence principles give different results on the same flow [11]. Unlike set-based approaches to coherent advective transport, the approach in [15] does not require diffusion barriers to be closed and hence also finds open bottlenecks to transport such as fronts and jets. This feature of the method is also important for closed diffusion barriers to remain detectable even if they do not lie entirely in the domain where velocity data is available.

While valid in arbitrary dimension, the results in [15] rely explicitly on the assumption that the flow carrying the concentration field of interest is incompressible. Liquid flows arising in applications are indeed practically incompressible, but air flows are relatively easy to compress. This precludes the application of [15] to atmospheric transport problems, such as the identification of temperature barriers surrounding the polar vortices (cf. [4, 6, 20, 32]). Notable compressibility also arises in two-dimensional velocity fields representing horizontal slices of planetary atmospheres, obtained from observations [12] or from numerical models [2]. The dramatic accumulation of oil and flotsam on the ocean surface [7], as well as the characteristically nonconservative surface patterns formed by algae [37], also necessitate the use of two-dimensional numerical models with significantly compressible, two-dimensional velocity fields.

These examples of compressible velocity fields nevertheless invariably conserve mass. For instance, oil remains buoyant and hence confined to the ocean surface, thus there is no significant loss in the total oil mass in the absence of other processes eroding it. Accordingly, a velocity field model for surface oil transport should be mass conserving. Inspired by such examples, we consider here diffusive transport in the presence of a carrier flow that may be compressible but conserves mass. At the same time, we also allow for variations of the transported concentration field due to effects beyond diffusion. These effects include contribution from distributed sources and sinks, as well as spontaneous concentration decay in time governed by a potentially time-dependent decay rate.

A number of prior approaches to weakly diffusive transport exist (see, e.g., [36] for a survey), but only a handful of these target structures in the compressible advection-diffusion equation. Among these, [33, 34] recast the advection-diffusion equation in Lagrangian coordinates and suggest a quasi-reduction to a one-dimensional diffusion PDE along the most contracting direction. While this approach yields formal asymptotic scaling laws for stretching and folding statistics along chaotic trajectories, such trajectories become undefined for finite-time data sets that we seek to analyze here. The residual velocity field of [27] offers

an attractive visualization tool for regions of enhanced or suppressed transport but requires already performed diffusive simulations as input, rather than providing predictions for them from velocity data (see also [1]). The popular effective diffusivity approach of [25] is based on the assumption of incompressibility (conservation of area) and hence becomes inapplicable to compressible flows. We finally mention recent work in [17] which provides an advection–diffusion interpretation for the compressible dynamic isoperimetry methodology developed in [10]. This latter, set-based approach targets metastable or almost-invariant sets in a purely advective transport context.

Our analysis here considers a mass-based (rather than volume-based) concentration field $c(\mathbf{x}, t)$. In the absence of diffusion, spontaneous concentration decay, and concentration sources, the transport of $c(\mathbf{x}, t)$ in and out of an evolving material volume $V(t)$ would be pointwise zero due to the conservation of the mass of $V(t)$ by the flow. Source terms and spontaneous concentration decay add a deterministic evolution to the concentration along particle trajectories, and hence the initial concentration remains deterministically reproducible, i.e., a conserved quantity along all particle motions in the absence of diffusion.

The presence of diffusion, however, erodes this conservation law, as if trajectories were stochastic and hence the value of the initial concentration along them could not be immediately reproduced just from the knowledge of the present concentration, the initial time, and the initial location along a fluid particle trajectory. Here, we will seek transport barriers as material surfaces across which this diffusive erosion of initial concentrations is stationary when compared to nearby material surfaces. For incompressible flows, this barrier concept will turn out to simplify exactly to the concept of most impermeable material barriers to diffusion, as developed in [15]. In the present work, we will collectively refer to stationary surfaces (minimizers, maximizers, and saddle-type surfaces) of diffusive transport as transport barriers without performing a second-order calculation to identify their types. As its prior incompressible version in [15], our present approach to transport barriers does not require them to be closed and hence applies to open barriers (such as fronts and jet cores) as well.

Beyond adding the effects of compressibility, sources, sinks, and spontaneous decay, our present analysis performs the transport extremization both with and without conditioning it on a known initial concentration field. In this context, unconstrained barriers are material surfaces that prevail as stationary surfaces of transport even under concentration gradients initially normal to them. Constrained barriers, in contrast, are stationary surfaces of transport under a fixed initial diffusion-gradient configuration. We derive mathematical criteria for both types of barriers and illustrate these criteria first on explicitly known Navier–Stokes flows, then on observational and numerical ocean data.

Our analysis and examples show that several well-documented features in a diffusing scalar field, such as jets and fronts, are technically not minimizers of diffusive transport when constrained on a given initial scalar field. This is at odds with the usual terminology by which surfaces of large concentration gradients are generally referred to as transport barriers, even though the actual transport through them appears large precisely because of those large gradients. This paradox has already been pointed out in the Eulerian frame but has remained unresolved [25]. Here we recover the same effect in rigorous terms in the Lagrangian frame and find that barriers are transport maximizers with respect to all localized perturbations.

2. Set-up. We consider the compressible advection-diffusion equation for a mass-unit-based concentration field $c(\mathbf{x}, t)$ in the general form

$$(2.1) \qquad \partial_t (\rho c) + \boldsymbol{\nabla} \cdot (\rho c \mathbf{v}) = \nu \boldsymbol{\nabla} \cdot (\rho \mathbf{D} \boldsymbol{\nabla} c) - k(t)\rho c + f(\mathbf{x}, t)\rho,$$
$$c(\mathbf{x}, t_0) = c_0(\mathbf{x}), \quad \rho(\mathbf{x}, t_0) = \rho_0(\mathbf{x}).$$

Here $\boldsymbol{\nabla}$ denotes the gradient operation with respect to the spatial variable $\mathbf{x} \in U \subset \mathbb{R}^n$ on a compact domain U with $n \geq 1$; $\mathbf{v}(\mathbf{x}, t)$ is an n-dimensional, spatially at least C^2-smooth (and hence shock-free), mass-conserving velocity field generating the advective transport of $c(\mathbf{x}, t)$ whose initial distribution is $c_0(\mathbf{x})$; $\mathbf{D}(\mathbf{x}, t) = \mathbf{D}^T(\mathbf{x}, t) \in \mathbb{R}^{n \times n}$ is a dimensionless, positive definite diffusion structure tensor describing possible inhomogeneity, anisotropy, and temporal variation in the diffusive transport of c; $\rho(\mathbf{x}, t) > 0$ is the mass-density of the carrier medium; $\nu \geq 0$ is a small diffusivity parameter rendering the full diffusion tensor $\nu \mathbf{D}$ small in norm; $k(\mathbf{x}, t)$ is a space- and time-dependent coefficient governing spontaneous concentration decay in the absence of diffusion; and $f(\mathbf{x}, t)$ describes the spatiotemporal sink and source distribution for the concentration. We assume that the initial concentration $c(\mathbf{x}, t_0) = c_0(\mathbf{x})$ is of class C^2, and $\mathbf{D}(\mathbf{x}, t)$, $k(t)$, and $f(\mathbf{x}, t)$ are at least Hölder-continuous, which certainly holds if they are continuously differentiable. We will therefore assume the latter for simplicity.

Without the spontaneous decay and source terms, (2.1) was apparently first obtained by Landau and Lifschitz [19] as a compressible, non-Fickian advection-diffusion equation for ρc (see also Thiffeault [34]). We note, however, that with the modified velocity field

$$(2.2) \qquad \mathbf{w} = \mathbf{v} + \frac{\nu}{\rho} \mathbf{D} \boldsymbol{\nabla} \rho,$$

(2.1) can also be recast as

$$(2.3) \qquad \partial_t (\rho c) + \boldsymbol{\nabla} \cdot (\rho c \mathbf{w}) = \nu \boldsymbol{\nabla} \cdot (\mathbf{D} \boldsymbol{\nabla} (\rho c)) - k(t)\rho c + f(\mathbf{x}, t)\rho,$$

an advection-diffusion equation with classic Fickian diffusion for the scalar field ρc under the modified velocity field $\mathbf{w}$.

Given a carrier velocity field $\mathbf{v}(\mathbf{x}, t)$ of general divergence $\nabla \cdot \mathbf{v}(\mathbf{x}, t)$, the density ρ featured in (2.1)–(2.3) must satisfy the equation of continuity

$$(2.4) \qquad \partial_t \rho + \boldsymbol{\nabla} \cdot (\rho \mathbf{v}) = 0.$$

Combining the continuity equation (2.4) with (2.1) gives an alternative form of the compressible advection-diffusion equation as

$$(2.5) \qquad \frac{Dc}{Dt} = \frac{1}{\rho} \nu \boldsymbol{\nabla} \cdot (\rho \mathbf{D} \boldsymbol{\nabla} c) - kc + f.$$

The flow map induced by the velocity field $\mathbf{v}$ is $\mathbf{F}_{t_0}^t : \mathbf{x}_0 \mapsto \mathbf{x}(t; t_0, \mathbf{x}_0)$, mapping initial positions $\mathbf{x}_0 \in U$ to their later positions at time t. We assume that all trajectories stay in the domain U of known velocities, i.e., $\mathbf{F}_{t_0}^t(U) \subset U$ holds for all times t of interest.[1] We will be

---

[1]This assumption still allows for the detection of subsets of a diffusion barrier that is not fully contained in U, as long as such subsets are formed by trajectories staying in U over the time interval $[t_0, t_1]$.

studying diffusive transport through *material surfaces* which are time-dependent families of codimension-one differentiable manifolds satisfying

$$\mathcal{M}(t) = \mathbf{F}_{t_0}^t(\mathcal{M}_0) \subset U,$$

with $\mathcal{M}(t_0) = \mathcal{M}_0$ denoting the initial position of the material surface. Note that $(\mathcal{M}(t), t)$ is an n-dimensional invariant manifold in the extended, $n+1$-dimensional phase space of the nonautonomous ODE $\dot{\mathbf{x}} = \mathbf{v}(\mathbf{x}, t)$.

We denote by $\boldsymbol{\nabla}_0 \mathbf{F}_{t_0}^t$ the gradient of $\mathbf{F}_{t_0}^t$ with respect to initial positions $\mathbf{x}_0$, satisfying

$$(2.6) \qquad \det \boldsymbol{\nabla}_0 \mathbf{F}_{t_0}^t(\mathbf{x}_0) = \exp \int_{t_0}^t \boldsymbol{\nabla} \cdot \mathbf{v}\left(\mathbf{F}_{t_0}^s(\mathbf{x}_0), s\right) ds.$$

The equation of continuity (2.4) together with (2.6) then yields the relation

$$\rho\left(\mathbf{F}_{t_0}^t(\mathbf{x}_0), t\right) = \rho_0(\mathbf{x}_0) \exp\left[-\int_{t_0}^t \boldsymbol{\nabla} \cdot \mathbf{v}\left(\mathbf{F}_{t_0}^s(\mathbf{x}_0), s\right) ds\right] = \frac{\rho_0(\mathbf{x}_0)}{\det \boldsymbol{\nabla}_0 \mathbf{F}_{t_0}^t(\mathbf{x}_0)}.$$

The smallness of the diffusivity parameter ν is not just a convenient mathematical assumption: most diffusive processes in nature have very small ν values (i.e., large Péclet numbers) associated with them (see, e.g., Weiss and Provenzale [36]). The smallness of ν, however, does not automatically allow for simple perturbation approaches, because (2.1) is a singularly perturbed PDE for such ν values.

3. The compressible diffusion barrier problem. To formulate the compressible diffusion barrier problem outlined in the introduction in precise terms, we first observe that for $\nu = 0$, (2.5) is solved by

$$c(\mathbf{x}, t) = e^{-\int_{t_0}^t k(s)ds} c_0(\mathbf{F}_t^{t_0}(\mathbf{x})) + \int_{t_0}^t e^{-\int_s^t k(\sigma)d\sigma} f(\mathbf{F}_t^s(\mathbf{x}), s) ds.$$

Therefore, the function

$$(3.1) \qquad \mu(\mathbf{x}, t) := e^{\int_{t_0}^t k(s)ds} c(\mathbf{x}, t) - \int_{t_0}^t e^{\int_{t_0}^s k(\sigma)d\sigma} f(\mathbf{F}_t^s(\mathbf{x}), s) ds,$$

returning the initial concentration at time t_0 along characteristics of (2.5), is conserved along trajectories (i.e., $\frac{D}{Dt}\mu(\mathbf{x}(t), t)) \equiv 0$), given that $\mu(\mathbf{x}(t), t) = c_0(\mathbf{F}_t^{t_0}(\mathbf{x})) \equiv c_0(\mathbf{x}_0)$.

For nonzero ν values, μ is no longer conserved along trajectories of $\mathbf{v}(\mathbf{x}, t)$. In that case, $\frac{D}{Dt}\mu(\mathbf{x}(t), t)$ measures the irreversibility in the evolution of $c(\mathbf{x}, t)$ along trajectories. Specifically, we have

$$\frac{D}{Dt}\mu(\mathbf{x}, t) = \frac{D}{Dt}\left[e^{\int_{t_0}^t k(s)ds} c(\mathbf{F}_{t_0}^t(\mathbf{x}_0), t) - \int_{t_0}^t e^{\int_{t_0}^s k(\sigma)d\sigma} f(\mathbf{F}_{t_0}^s(\mathbf{x}_0), s) ds\right]$$

$$= k(t)e^{\int_{t_0}^t k(s)ds} c\left(\mathbf{F}_{t_0}^t(\mathbf{x}_0), t\right) + e^{\int_{t_0}^t k(s)ds}\frac{D}{Dt}c\left(\mathbf{F}_{t_0}^t(\mathbf{x}_0), t\right) - e^{\int_{t_0}^t k(s)ds} f\left(\mathbf{F}_{t_0}^t(\mathbf{x}_0), t\right)$$

$$(3.2) \qquad = \nu\frac{1}{\rho(\mathbf{x}, t)}\boldsymbol{\nabla}\cdot\left(\rho(\mathbf{x}, t)\mathbf{D}(\mathbf{x}, t)\boldsymbol{\nabla}\left[\mu(\mathbf{x}, t) + \int_{t_0}^t e^{\int_{t_0}^s k(\sigma)d\sigma} f(\mathbf{F}_t^s(\mathbf{x}), s) ds\right]\right).$$

This latter PDE for the evolution of $\mu(\mathbf{x}, t)$ can also be rewritten in Lagrangian coordinates applying the formulas of Tang and Boozer [33] and Thiffeault [34] that transform the classic advection-diffusion equation to Lagrangian coordinates. When applied to $\hat{\mu}(\mathbf{x}_0, t) := \mu(\mathbf{F}_{t_0}^t(\mathbf{x}_0), t)$, those formulas directly give

$$(3.3) \qquad \partial_t \hat{\mu}(\mathbf{x}_0, t) = \nu \frac{1}{\rho_0(\mathbf{x}_0)} \boldsymbol{\nabla}_0 \cdot \left(\mathbf{T}_{t_0}^t(\mathbf{x}_0) \boldsymbol{\nabla}_0 \left[\hat{\mu}(\mathbf{x}_0, t) + b(\mathbf{x}_0, t) \right] \right),$$

where $\boldsymbol{\nabla}_0$ denotes the spatial gradient with respect to the initial condition $\mathbf{x}_0$, and $\mathbf{T}_{t_0}^t$ and $b(\mathbf{x}_0, t)$ are defined as

$$(3.4) \qquad \mathbf{T}_{t_0}^t(\mathbf{x}_0) := \rho_0(\mathbf{x}_0) \left[\boldsymbol{\nabla}_0 \mathbf{F}_{t_0}^t(\mathbf{x}_0) \right]^{-1} \mathbf{D}(\mathbf{F}_{t_0}^t(\mathbf{x}_0), t) \left[\boldsymbol{\nabla}_0 \mathbf{F}_{t_0}^t(\mathbf{x}_0) \right]^{-T},$$

$$b(\mathbf{x}_0, t) := \int_{t_0}^t e^{\int_{t_0}^s k(\sigma) d\sigma} f(\mathbf{F}_{t_0}^s(\mathbf{x}_0), s) \, ds.$$

The definition of the *transport tensor* $\mathbf{T}_{t_0}^t(\mathbf{x}_0)$ in (3.4) is similar to that in [15] but the present definition also contains the initial density $\rho_0(\mathbf{x}_0)$ as a factor and no longer assumes the flow map to be volume-preserving.

Remark 1. It will be crucial in our present derivation that no spatially dependent terms beyond the initial density remain in front of the divergence operation in (3.2). That is the case only if the flow map of the characteristics of (2.1) is linear in $\mathbf{x}_0$ for $\nu = 0$. This, in turn, holds only if the right-hand side of (2.1) is a linear function of $c(\mathbf{x}, t)$ with a spatially independent function $k(t)$, as we have assumed. Consequently, (2.1) is the broadest class of PDEs to which our present approach is applicable.

The following result is critical to our analysis, establishing a leading-order formula for the total transport

$$\Sigma_{t_0}^{t_1}(\mathcal{M}_0) = \nu \int_{t_0}^{t_1} \int_{\mathcal{M}(t)} \rho(\mathbf{x}, t) \left\langle \mathbf{D}(\mathbf{x}, t) \boldsymbol{\nabla} \left[\mu(\mathbf{x}, t) + \int_{t_0}^t e^{\int_{t_0}^s k(\sigma) d\sigma} f(\mathbf{F}_t^s(\mathbf{x}), s) \, ds \right], \mathbf{n} \right\rangle dA dt$$

of the scalar field $\mu(x, t)$ field through an evolving material surface $\mathcal{M}(t)$, where we have deduced the expression of the pertinent flux vector for $\Sigma_{t_0}^{t_1}(\mathcal{M}_0)$ from (3.2).

Theorem 1. *The total transport $\Sigma_{t_0}^{t_1}(\mathcal{M}_0)$ of μ through an arbitrary, evolving material surface $\mathcal{M}(t) = \mathbf{F}_{t_0}^t(\mathcal{M}_0)$ over the time interval $[t_0, t_1]$ is given by*

$$(3.5) \qquad \Sigma_{t_0}^{t_1}(\mathcal{M}_0) = \nu \int_{t_0}^{t_1} \int_{\mathcal{M}_0} \left\langle \mathbf{T}_{t_0}^t \left(\boldsymbol{\nabla}_0 c_0(\mathbf{x}_0) + \boldsymbol{\nabla}_0 b(\mathbf{x}_0,) \right), \mathbf{n}_0 \right\rangle dA_0 dt + o(\nu)$$

with $\langle \cdot, \cdot \rangle$ denoting the Euclidean inner product, dA_0 denoting the surface element along the initial material surface $\mathcal{M}_0$, and $o(\nu)$ denoting a quantity that, for $\nu \to 0$, tends to 0 even after division by ν.

Proof. See Appendix A. ∎

Next, we will seek diffusion barriers as codimension-one stationary surfaces of the leading-order term in the expression of $\Sigma_{t_0}^{t_1}(\mathcal{M}_0)$ in two different settings. First, we consider the

initial tracer concentration unknown or uncertain, and assume the most diffusion-prone initial concentration distribution for c along each material surface. Next, we consider an arbitrary but fixed initial concentration and seek material surfaces that render diffusive transport stationary under this initial concentration.

4. Unconstrained diffusion barriers. To compare the intrinsic ability of different material surfaces to withstand diffusion, we now subject each material surface to the same, locally customized initial concentration gradient setting that makes the surface a priori maximally conducive to diffusive transport. Specifically, we fix two constants, $K_0 > 0$ and $\alpha \in (0, 1)$, and initialize the initial concentration along the initial position $\mathcal{M}_0$ of any material surface in such a way that

$$(4.1) \qquad \boldsymbol{\nabla}_0 c_0(\mathbf{x}_0) = \frac{K_0}{\nu^\alpha} \mathbf{n}_0(\mathbf{x}_0), \quad \nu > 0, \quad \mathbf{x}_0 \in \mathcal{M}_0.$$

In other words, we prescribe uniformly high concentration gradients along $\mathcal{M}_0$ that are perfectly aligned with the normals of $\mathcal{M}_0$ and grow as $\nu^{-\alpha}$ as $\nu \to 0$. We will refer to (4.1) as the *uniformity assumption.* This assumption focuses our analysis on the intrinsic ability of a material surface to block diffusion, rather than on its position relative to features present in a specific initial concentration field.

Remark 2. The uniformity assumption in [15] is a specific case of (4.1) with $\alpha = 0$. If sinks and sources are absent ($f(\mathbf{x}, t) \equiv 0$), as is the case in [15], we can also select $\alpha = 0$ in (4.1) and still obtain the upcoming results of this section.

By the compactness of U and the time interval $[t_0, t_1]$, we can also select a constant bound $M_0 > 0$ so that

$$(t_1 - t_0) \left| \int_{t_0}^{t_1} \boldsymbol{\nabla}_0 \left[\frac{1}{\rho_0(\mathbf{x}_0)} \boldsymbol{\nabla}_0 \cdot \left(\mathbf{T}_{t_0}^s(\mathbf{x}_0) \boldsymbol{\nabla}_0 b(\mathbf{x}_0, s) \right) \right] ds \right| \le M_0$$

for all $\mathbf{x}_0 \in U$, given that $\mathbf{T}_{t_0}^s(\mathbf{x}_0) \boldsymbol{\nabla}_0 b(\mathbf{x}_0, s)$ is assumed C^1 for all s values. We can then rewrite $\Sigma_{t_0}^{t_1}(\mathcal{M}_0)$ in (3.5) as

$$\Sigma_{t_0}^{t_1}(\mathcal{M}_0) = \nu(t_1 - t_0) K_0 \int_{\mathcal{M}_0} \left\langle \bar{\mathbf{T}}_{t_0}^{t_1} \mathbf{n}_0, \mathbf{n}_0 \right\rangle dA_0 + o(\nu) + \mathcal{O}\left(\nu \frac{M_0 \rho_0 \nu^\alpha}{K_0} \right).$$

This leads to the normalized total transport of $\mu(\mathbf{x}, t)$ in the form

$$(4.2) \qquad \widetilde{\Sigma}_{t_0}^{t_1}(\mathcal{M}_0) := \frac{\Sigma_{t_0}^{t_1}(\mathcal{M}_0)}{\nu K_0 (t_1 - t_0) A_0(\mathcal{M}_0)} = \mathcal{T}_{t_0}^{t_1}(\mathcal{M}_0) + o(\nu^\alpha), \quad \alpha \in (0, 1],$$

where the *transport functional,*

$$(4.3) \qquad \mathcal{T}_{t_0}^{t_1}(\mathcal{M}_0) := \frac{\int_{\mathcal{M}_0} \left\langle \mathbf{n}_0, \bar{\mathbf{T}}_{t_0}^{t_1} \mathbf{n}_0 \right\rangle dA_0}{\int_{\mathcal{M}_0} dA_0},$$

measures the leading-order diffusive transport of $c(\mathbf{x}, t)$ through the material surface $\mathcal{M}(t)$ over the period $[t_0, t_1]$. This functional formally coincides with the transport functional obtained in [15] for incompressible flows with $k(t) \equiv f(\mathbf{x}, t) \equiv 0$ in the PDE (2.1). The only,

minor, difference here is in the definition (3.4) of $\bar{\mathbf{T}}_{t_0}^{t_1}$, which now features the initial density field $\rho_0(\mathbf{x}_0)$. Importantly, the present theory returns the results of the incompressible theory when applied to incompressible flows with uniform density. We stress that $\mathcal{T}_{t_0}^{t_1}(\mathcal{M}_0)$ can be computed for any initial surface $\mathcal{M}_0$ directly from the trajectories of $\mathbf{v}$ without solving the PDE (2.1).

We propose that what makes a barrier most observable is a near-uniform concentration jump along it. By continuity with respect to all quantities involved over finite time intervals, however, surfaces delineating near-uniform concentration jumps form continuous families and hence cannot be uniquely identified. The theoretical centerpiece of such a family is still well defined by *uniform barriers* which are characterized by constant pointwise transport density at leading order. By formula (4.3), these surfaces satisfy

$$(4.4) \qquad \langle \mathbf{n}_0, \bar{\mathbf{T}}_{t_0}^{t_1} \mathbf{n}_0 \rangle = \mathcal{T}_0 = \text{const.},$$

where the constant $\mathcal{T}_0 > 0$ is the constant diffusive transport density across each point of a uniform transport barrier $\mathcal{M}_0$.

Because of the formal coincidence between the transport functional $\mathcal{T}_{t_0}^{t_1}(\mathcal{M}_0)$ defined in (4.3) and that arising in the incompressible case, the general necessary criterion of [15] for uniform barriers remains valid here and can be stated with the help of the tensor family

$$(4.5) \qquad \mathbf{E}_{\mathcal{T}_0}(\mathbf{x}_0) := \bar{\mathbf{T}}_{t_0}^{t_1} - \mathcal{T}_0 \mathbf{I}$$

as follows.

Theorem 2. *Under assumption* (4.1), *a uniform minimizer $\mathcal{M}_0$ of the transport functional $\mathcal{T}_{t_0}^{t_1}$, with pointwise transport density $\mathcal{T}_0 > 0$, is necessarily a nonnegatively traced null-surface of the tensor field $\mathbf{E}_{\mathcal{T}_0}$, i.e.,*

$$(4.6) \qquad \langle \mathbf{n}_0(\mathbf{x}_0), \mathbf{E}_{\mathcal{T}_0}(\mathbf{x}_0)\mathbf{n}_0(\mathbf{x}_0) \rangle = 0, \qquad \text{trace}\, \mathbf{E}_{\mathcal{T}_0}(\mathbf{x}_0) \geq 0,$$

holds at every point $\mathbf{x}_0 \in \mathcal{M}_0$ with unit normal $\mathbf{n}_0(\mathbf{x}_0)$ to $\mathcal{M}_0$. Similarly, a uniform maximizer $\mathcal{M}_0$ of $\mathcal{T}_{t_0}^{t_1}$ is necessarily a nonpositively traced null-surface of the tensor field $\mathbf{E}_{\mathcal{T}_0}$, i.e.,

$$(4.7) \qquad \langle \mathbf{n}_0(\mathbf{x}_0), \mathbf{E}_{\mathcal{T}_0}(\mathbf{x}_0)\mathbf{n}_0(\mathbf{x}_0) \rangle = 0, \qquad \text{trace}\, \mathbf{E}_{\mathcal{T}_0}(\mathbf{x}_0) \leq 0,$$

holds at every point $\mathbf{x}_0 \in \mathcal{M}_0$.

Finally, by direct analogy with the incompressible case treated in [15], a diagnostic field measuring the strength of unconstrained diffusion barriers is given by the diffusion barriers strength (DBS) field, defined as

$$(4.8) \qquad DBS_{t_0}^{t_1}(\mathbf{x}_0) = \text{trace}\, \bar{\mathbf{T}}_{t_0}^{t_1}(\mathbf{x}_0).$$

This follows because, as shown in [15], the leading-order change in the nondimensionalized transport functional $\mathcal{T}_{t_0}^{t_1}$ under a small, surface-area-preserving perturbation localized in an $\mathcal{O}(\epsilon)$ neighborhood of a point $\mathbf{x}_0 \in \mathcal{M}_0$ is given by $\epsilon DBS_{t_0}^{t_1}(\mathbf{x}_0)$. Of all uniform extremizers, therefore, those along the ridges of $\left| DBS_{t_0}^{t_1}(\mathbf{x}_0) \right|$ will prevail as the strongest inhibitors or enhancers of diffusive transport.

4.1. Relationship between diffusion barriers and classic invariant manifolds.

In steady, temporally periodic or quasiperiodic flows known for infinite times, one expects classical invariant manifolds known as advective transport barriers to play a role in shaping the evolution of diffusive tracers as well. Here we examine what types of invariant manifolds become uniform diffusion barriers asymptotically in time.

Assume that the diffusion structure tensor is $\mathbf{D} \equiv \mathbf{I}$ (homogeneous and isotropic diffusion), $\rho_0(\mathbf{x}_0) = \rho_0 = \text{const.}$ (homogeneous initial density), and the conservation law (4.4) holds for $t_1 \in (t_0, \infty)$ over the material surface evolving from $\mathcal{M}_0$ under the flow map. This implies

$$\left\langle \mathbf{n}_0, \left(\frac{1}{t_1 - t_0} \int_{t_0}^{t_1} \rho_0 \left[\boldsymbol{\nabla}_0 \mathbf{F}_{t_0}^t(\mathbf{x}_0) \right]^{-1} \left[\boldsymbol{\nabla}_0 \mathbf{F}_{t_0}^t(\mathbf{x}_0) \right]^{-T} dt \right) \mathbf{n}_0 \right\rangle = \mathcal{T}_0,$$

or, equivalently,

$$\frac{1}{t_1 - t_0} \int_{t_0}^{t_1} \left| \left[\boldsymbol{\nabla}_0 \mathbf{F}_{t_0}^t(\mathbf{x}_0) \right]^{-T} \mathbf{n}_0(\mathbf{x}_0) \right|^2 dt = \frac{\mathcal{T}_0}{\rho_0} = \text{const.}, \qquad t_1 \in (t_0, \infty).$$

At the same time, the normal component of an initially normal unit perturbation to $\mathcal{M}_0$, represented by $\mathbf{n}_0(\mathbf{x}_0)$, is given by the orthogonal projection of the advected normal $\boldsymbol{\nabla}_0 \mathbf{F}_{t_0}^t(\mathbf{x}_0) \mathbf{n}_0(\mathbf{x}_0)$ onto the unit normal

$$\mathbf{n}\left(\mathbf{F}_{t_0}^t(\mathbf{x}_0) \right) = \frac{\left[\boldsymbol{\nabla}_0 \mathbf{F}_{t_0}^t(\mathbf{x}_0) \right]^{-T} \mathbf{n}_0(\mathbf{x}_0)}{\left| \left[\boldsymbol{\nabla}_0 \mathbf{F}_{t_0}^t(\mathbf{x}_0) \right]^{-T} \mathbf{n}_0(\mathbf{x}_0) \right|},$$

i.e., by the the normal repulsion rate $\sigma_{t_0}^t(\mathbf{x}_0)$, computed as

$$\sigma_{t_0}^t(\mathbf{x}_0) = \left\langle \boldsymbol{\nabla}_0 \mathbf{F}_{t_0}^t(\mathbf{x}_0) \mathbf{n}_0(\mathbf{x}_0), \frac{\left[\boldsymbol{\nabla}_0 \mathbf{F}_{t_0}^t(\mathbf{x}_0) \right]^{-T} \mathbf{n}_0(\mathbf{x}_0)}{\left| \left[\boldsymbol{\nabla}_0 \mathbf{F}_{t_0}^t(\mathbf{x}_0) \right]^{-T} \mathbf{n}_0(\mathbf{x}_0) \right|} \right\rangle$$

$$= \frac{1}{\left| \left[\boldsymbol{\nabla}_0 \mathbf{F}_{t_0}^t(\mathbf{x}_0) \right]^{-T} \mathbf{n}_0(\mathbf{x}_0) \right|}.$$

Therefore, we have

$$\frac{1}{t_1 - t_0} \int_{t_0}^{t_1} \frac{1}{\left[\sigma_{t_0}^t(\mathbf{x}_0) \right]^2} dt = \frac{\mathcal{T}_0}{\rho_0} = \text{const.},$$

or, equivalently,

$$\left\| \sigma_{t_0}^t(\mathbf{x}_0)^{-1} \right\|_{L^2(t_0, t_1)} = \frac{\mathcal{T}_0}{\rho_0} = \text{const.}$$

This shows that the temporally L^2-normed reciprocal of the normal stretching rate along the manifold $\mathcal{M}_0$ should be spatially constant along diffusion barriers. This is certainly satisfied for $t_1 \to \infty$ along stable manifolds of fixed points and periodic orbits, as well as along quasiperiodic invariant tori.

4.2. Unconstrained diffusion barriers in two-dimensional flows. In arbitrary dimensions, the first equation defining null-surfaces in (4.6) and (4.7) are PDEs with a priori unknown solvability properties. For two-dimensional flows, however, the null-surfaces become curves satisfying ODEs that turn out to be explicitly solvable (cf. [15]). These differential equations can be expressed in terms of the invariants of the time-averaged, diffusion-structure-weighted Cauchy–Green strain tensor

$$\bar{\mathbf{C}}_{\mathbf{D}}(\mathbf{x}_0) := \frac{1}{t_1 - t_0} \int_{t_0}^{t_1} \det\left[\mathbf{D}\left(\mathbf{F}_{t_0}^t(\mathbf{x}_0), t\right)\right] \left[\mathbf{T}_{t_0}^t(\mathbf{x}_0)\right]^{-1} dt$$

as follows.

Theorem 3. *For two-dimensional flows ($n = 2$), let $\boldsymbol{\xi}_i(\mathbf{x}_0) \in \mathbb{R}^2$ denote the unit eigenvectors corresponding to the eigenvalues $0 < \lambda_1(\mathbf{x}_0) \leq \lambda_2(\mathbf{x}_0)$ of the positive definite tensor $\bar{\mathbf{C}}_{\mathbf{D}}(\mathbf{x}_0)$. A uniform extremizer $\mathcal{M}_0$ of the transport functional $\mathcal{T}_{t_0}^{t_1}$, with pointwise transport density $\mathcal{T}_0 > 0$, is then necessarily a trajectory of the direction field family*

$$(4.9) \quad \mathbf{x}_0' = \boldsymbol{\eta}_{\mathcal{T}_0}^{\pm}(\mathbf{x}_0) := \sqrt{\frac{\lambda_2(\mathbf{x}_0) - \mathcal{T}_0}{\lambda_2(\mathbf{x}_0) - \lambda_1(\mathbf{x}_0)}} \boldsymbol{\xi}_1(\mathbf{x}_0) \pm \sqrt{\frac{\mathcal{T}_0 - \lambda_1(\mathbf{x}_0)}{\lambda_2(\mathbf{x}_0) - \lambda_1(\mathbf{x}_0)}} \boldsymbol{\xi}_2(\mathbf{x}_0), \qquad \mathbf{x}_0 \in U_{\mathcal{T}_0},$$

defined on the spatial domain $U_{\mathcal{T}_0} = \{\mathbf{x}_0 \in U : \lambda_1(\mathbf{x}_0) \leq \mathcal{T}_0 \leq \lambda(\mathbf{x}_0), \ \lambda_2(\mathbf{x}_0) \neq \lambda_1(\mathbf{x}_0)\}$.

The domain of definition $U_{\mathcal{T}_0} \subset U$ of the direction field family $\boldsymbol{\eta}_{\mathcal{T}_0}^{\pm}(\mathbf{x}_0)$ is precisely the spatial domain where the tensor field $\mathbf{E}_{\mathcal{T}_0}$ defined in (4.5) is indefinite (Lorentzian) and hence indeed has well-defined null-surfaces. The set $U_{\mathcal{T}_0}$ will depend on the value of the parameter $\mathcal{T}_0$ and will be a nonempty subset of U for any $\mathcal{T}_0 \in \left[\inf_{\mathbf{x}_0 \in U} \lambda_1(\mathbf{x}_0), \sup_{\mathbf{x}_0 \in U} \lambda_2(\mathbf{x}_0)\right]$. For $\mathcal{T}_0$ values outside this interval, $U_{\mathcal{T}_0}$ will be an empty set, which means that there will be no barriers with such transport density $\mathcal{T}_0$ in the domain U. Formula (4.9) enables a detailed computation of diffusion barriers in two dimensions based on a numerical approximation of the flow map $\mathbf{F}_{t_0}^t(\mathbf{x}_0)$ obtained on a grid of initial conditions (see [15] for details).

The direction field $\boldsymbol{\eta}_{\mathcal{T}_0}^{\pm}(\mathbf{x}_0)$ is as smooth as the eigenvalues $\lambda_i(\mathbf{x}_0)$, given that no repeated eigenvalues can arise within $U_{\mathcal{T}_0}$ by its definition. The eigenvalues $\lambda_i(\mathbf{x}_0)$ are, in turn, as smooth as the transport tensor $\mathbf{T}_{t_0}^t(\mathbf{x}_0)$, which is one degree less smooth than the class C^2 vector field $\mathbf{v}(\mathbf{x}, t)$ by the smooth dependence of the flow map $\mathbf{F}_{t_0}^t$ on $\mathbf{x}_0$, and by the assumed smooth dependence of the diffusivity structure tensor $\mathbf{D}$ on $\mathbf{x}_0$. Therefore, $\boldsymbol{\eta}_{\mathcal{T}_0}^{\pm}(\mathbf{x}_0)$ is a class C^1 direction field and hence can always be locally oriented to become a class C^1 vector field. Consequently, $\boldsymbol{\eta}_{\mathcal{T}_0}^{\pm}(\mathbf{x}_0)$ will always have locally well-defined trajectories starting from any initial condition in $U_{\mathcal{T}_0}$. All these trajectories are uniform transport barriers of the same pointwise transport density $\mathcal{T}_0$ by construction. Not all these trajectories are, however, equally observable barriers. Some stand out because of their topology (e.g., they are closed), others because of their strength due to high DBS values along them.

As shown in [15] for two-dimensional flows, we have $\bar{\mathbf{T}}_{t_0}^{t_1} = \det\left(\bar{\mathbf{C}}_{\mathbf{D}}\right) \bar{\mathbf{C}}_{\mathbf{D}}^{-1}$. This implies that the DBS field defined in (4.8) in the present, two-dimensional case can be evaluated as

$$(4.10) \qquad DBS_{t_0}^{t_1}(\mathbf{x}_0) = \text{trace } \bar{\mathbf{T}}_{t_0}^{t_1}(\mathbf{x}_0) = \det \bar{\mathbf{C}}_{\mathbf{D}}(\mathbf{x}_0)\text{trace } \bar{\mathbf{C}}_{\mathbf{D}}^{-1}(\mathbf{x}_0) = \text{trace } \bar{\mathbf{C}}_{\mathbf{D}}(\mathbf{x}_0).$$

The results in Theorems 1 and 2 are directly applicable to incompressible flows as well, in which case they agree with the results in [15]. The derivation in [15], however, does not apply to the present, compressible case, while our argument leading to the normalized total transport $\widetilde{\Sigma}_{t_0}^{t_1}(\mathcal{M}_0)$ in (4.2) is general enough to cover the incompressible case as well.

5. Constrained diffusion extremizers. The above formulation is independent of the initial concentration $c_0(\mathbf{x})$ and assumes large enough initial gradients along the initial surface $\mathcal{M}_0$ that continue to dominate contributions from concentration decay and source terms (cf. the uniformity assumption (4.1)). If, however, we wish to extremize diffusive transport with respect to a specific initial concentration field $c_0(\mathbf{x}_0)$, as opposed to unspecified or uncertain initial concentrations, then we can no longer prescribe (4.1) along an arbitrary material surface $\mathcal{M}_0$. Indeed, some material surfaces will experience $\boldsymbol{\nabla}_0 c_0$ vectors favorable to cross-surface diffusion while others will not.

Considering $\boldsymbol{\nabla}_0 c_0$ as a given quantity and using formula (3.5), we rewrite the normed, total transport of $\mu(\mathbf{x}, t)$ as

$$\widetilde{\Sigma}_{t_0}^{t_1}(\mathcal{M}_0) := \frac{1}{\int_{\mathcal{M}_0} dA_0} \int_{t_0}^{t_1} \int_{\partial V(t_0)} \left\langle \mathbf{T}_{t_0}^s \left(\boldsymbol{\nabla}_0 c(\mathbf{x}_0) + \boldsymbol{\nabla}_0 b(\mathbf{x}_0, s) \right), \mathbf{n}_0 \right\rangle \, dA_0 ds + o(\nu^\alpha)$$

$$(5.1) \qquad = \frac{\int_{\mathcal{M}_0} \left\langle \bar{\mathbf{q}}_{t_0}^{t_1}, \mathbf{n}_0 \right\rangle \, dA_0}{\int_{\mathcal{M}_0} dA_0} + o(\nu^\alpha)$$

with the help of the *transport vector field*

$$(5.2) \qquad \bar{\mathbf{q}}_{t_0}^{t_1}(\mathbf{x}_0) := \int_{t_0}^{t_1} \left[\mathbf{T}_{t_0}^t(\mathbf{x}_0) \left(\boldsymbol{\nabla}_0 c_0(\mathbf{x}_0) + \boldsymbol{\nabla}_0 b(\mathbf{x}_0, t) \right) \right] dt.$$

The sign of the net total transport $\widetilde{\Sigma}_{t_0}^{t_1}(\mathcal{M}_0)$ through $\mathcal{M}_0$ is now not necessarily positive, which necessitates extremizing the normed transport (the time-integral of the geometric flux in the terminology of MacKay [23]). To this end, we seek to extremize the area-normalized, leading-order, normed diffusive transport

$$\widetilde{\mathcal{E}}(\mathcal{M}_0) := \frac{\int_{\mathcal{M}_0} \left| \left\langle \bar{\mathbf{q}}_{t_0}^s, \mathbf{n}_0 \right\rangle \right| \, dA_0}{\int_{\mathcal{M}_0} dA_0}$$

with respect to the initial surface $\mathcal{M}_0$, for which a necessary condition is the vanishing first variation,

$$(5.3) \qquad \delta \widetilde{\mathcal{E}}(\mathcal{M}_0) = 0,$$

with the derivative of $\widetilde{\mathcal{E}}$ taken at $\mathcal{M}_0$ with respect to a smooth, one-parameter family of material surfaces containing $\mathcal{M}_0$. For such stationary surfaces of $\widetilde{\mathcal{E}}$, we have the following result.

Theorem 4. *Along any solution $\mathcal{M}_0$ of the variational problem* (5.3), *there exists a constant $C \in \mathbb{R}$ such that*

$$\left[\left| \left\langle \bar{\mathbf{q}}_{t_0}^{t_1}(\mathbf{x}_0), \mathbf{n}_0 \left(\partial_{\mathbf{s}} \mathbf{x}_0 \right) \right\rangle \right| - \mathcal{T}_0 \right] \sqrt{\det \mathbf{G} \left(\partial_{\mathbf{s}} \mathbf{x}_0 \right)} = C, \qquad \mathbf{x}_0 \in \mathcal{M}_0,$$

with $\mathcal{T}_0 := \widetilde{\mathcal{E}}(\mathcal{M}_0)$ denoting the value of the normed transport functional on $\mathcal{M}_0$.

Proof. See Appendix B. ∎

As argued in [15], the most observable stationary surfaces of diffusive transport are those with nearly uniformly high gradients along them, associated with a nearly uniform pointwise transport density. The theoretical centerpieces of such regions are provided by surfaces with perfectly uniform transport density, which, by the statement of Theorem 4 with $C = 0$, satisfy the implicit equation

$$(5.4) \qquad \left| \left\langle \bar{\mathbf{q}}_{t_0}^{t_1}(\mathbf{x}_0(\mathbf{s})), \mathbf{n}_0(\partial_\mathbf{s}\mathbf{x}_0(\mathbf{s})) \right\rangle \right| = \mathcal{T}_0$$

for any selected pointwise transport density $\mathcal{T}_0 \geq 0$.

Remark 3. By analogy with the DBS field defined in (4.8), a direct measure of the local strength of a uniform constrained barrier is

$$(5.5) \qquad DBS_{t_0}^{t_1}(\mathbf{x}_0) = \left| \bar{\mathbf{q}}_{t_0}^{t_1}(\mathbf{x}_0) \right|,$$

a predictive diagnostic field applicable in any dimension. This diagnostic emerges as the normed, leading-order change in the functional $\mathcal{E}(\mathcal{M}_0)$ under small, localized perturbations to a stationary surface $\mathcal{M}_0$. Ridges of $DBS_{t_0}^{t_1}(\mathbf{x}_0)$ are expected to highlight the strongest diffusive transport barriers over the time interval $[t_0, t_1]$.

Remark 4. When $k(t) \equiv 0$ and $f(\mathbf{x}, t) \equiv 0$ holds (no sources or sinks), then we have $\hat{\mu}(\mathbf{x}_0, t) \equiv c(\mathbf{F}_{t_0}^t(\mathbf{x}_0), t)$ and $\widetilde{\Sigma}_{t_0}^{t_1}(\mathcal{M}_0)$ in (5.1) can exactly—i.e., without the $o(\nu)$ error—be represented as

$$(5.6) \qquad \widetilde{\Sigma}_{t_0}^{t_1}(\mathcal{M}_0) = \nu \frac{1}{\int_{\mathcal{M}_0} dA_0} \int_{t_0}^{t_1} \int_{\mathcal{M}_0} \left\langle \mathbf{T}_{t_0}^t(\mathbf{x}_0) \boldsymbol{\nabla}_0 c(\mathbf{F}_{t_0}^t(\mathbf{x}_0), t), \mathbf{n}_0(\mathbf{x}_0) \right\rangle \, dA_0 \, dt,$$

as ones verifies from (A.4) in Appendix A. Furthermore, noting that in this case $\hat{\mu}(\mathbf{x}_0, t) \equiv c(\mathbf{F}_{t_0}^t(\mathbf{x}_0), t)$, we obtain from the chain rule that

$$\mathbf{T}_{t_0}^t(\mathbf{x}_0) \boldsymbol{\nabla}_0 c(\mathbf{F}_{t_0}^t(\mathbf{x}_0), t) = \rho_0(\mathbf{x}_0) \left[\boldsymbol{\nabla}_0 \mathbf{F}_{t_0}^t(\mathbf{x}_0) \right]^{-1} \mathbf{D}(\mathbf{F}_{t_0}^t(\mathbf{x}_0), t) \left[\boldsymbol{\nabla}_0 \mathbf{F}_{t_0}^t(\mathbf{x}_0) \right]^{-T} \boldsymbol{\nabla}_0 c(\mathbf{F}_{t_0}^t(\mathbf{x}_0), t)$$

$$(5.7) \qquad = \rho_0(\mathbf{x}_0) \left[\boldsymbol{\nabla}_0 \mathbf{F}_{t_0}^t(\mathbf{x}_0) \right]^{-1} \mathbf{D}(\mathbf{F}_{t_0}^t(\mathbf{x}_0), t) \boldsymbol{\nabla} c(\mathbf{F}_{t_0}^t(\mathbf{x}_0), t).$$

Therefore, formulas (5.6)–(5.7) give an exact expression for $\widetilde{\Sigma}_{t_0}^{t_1}(\mathcal{M}_0)$ with a redefined form of $\bar{\mathbf{q}}_{t_0}^{t_1}$ as

$$\widetilde{\Sigma}_{t_0}^{t_1}(\mathcal{M}_0) := \frac{\int_{\mathcal{M}_0} \left\langle \bar{\mathbf{q}}_{t_0}^{t_1}, \mathbf{n}_0 \right\rangle \, dA_0}{\int_{\mathcal{M}_0} dA_0},$$

$$(5.8) \qquad \bar{\mathbf{q}}_{t_0}^{t_1}(\mathbf{x}_0) := \int_{t_0}^{t_1} \rho_0(\mathbf{x}_0) \left[\boldsymbol{\nabla}_0 \mathbf{F}_{t_0}^t(\mathbf{x}_0) \right]^{-1} \mathbf{D}(\mathbf{F}_{t_0}^t(\mathbf{x}_0), t) \boldsymbol{\nabla} c(\mathbf{F}_{t_0}^t(\mathbf{x}_0), t) \, dt.$$

Using the form (5.8) of $\bar{\mathbf{q}}_{t_0}^{t_1}(\mathbf{x}_0)$ in all our results below increases the accuracy of transport extremizer detection. At the same time, formula (5.8) requires explicit knowledge of the current concentration $c(\mathbf{x}, t)$, which generally necessitates the numerical solution of the advection-diffusion equation (2.1). A notable case in which (5.8) is useful is when $c(\mathbf{x}, t) = \omega(\mathbf{x}, t)$

is the scalar vorticity associated with a two-dimensional velocity field $\mathbf{v}(\mathbf{x}, t)$. In that case, once $\mathbf{v}(\mathbf{x}, t)$ is known, $\omega(\mathbf{x}, t)$ is readily obtained as the plane-normal component of $\nabla\omega(\mathbf{x}, t)$ without the need to solve the vorticity-transport equation. In this latter case, no assumption is needed on the smallness of the viscosity ν.

5.1. Perfect constrained barriers and enhancers to diffusion. In any dimension, a distinguished subset of uniform constrained barriers, the *perfect barriers,* inhibit transport completely pointwise at leading order, i.e., are characterized by $\mathcal{T}_0 = 0$. By (5.4), the time-t_0 positions of perfect constrained barriers satisfy

$$(5.9) \qquad \left\langle \bar{\mathbf{q}}_{t_0}^{t_1}, \mathbf{n}_0 \right\rangle = 0.$$

Therefore, the vector $\bar{\mathbf{q}}_{t_0}^{t_1}(\mathbf{x}_0)$ is necessarily tangent to a perfect barrier at every point $\mathbf{x}_0$. In other words, time-t_0 positions of material surfaces acting as perfect constrained material barriers to diffusive transport are necessarily codimension-one invariant manifolds of the autonomous dynamical system

$$(5.10) \qquad \mathbf{x}_0' = \bar{\mathbf{q}}_{t_0}^{t_1}(\mathbf{x}_0) = \bar{\mathbf{T}}_{t_0}^{t_1}(\mathbf{x}_0)\,\nabla_0 c_0(\mathbf{x}_0) + \bar{\mathbf{B}}_{t_0}^{t_1}(\mathbf{x}_0), \qquad \mathbf{x}_0 \in U \subset \mathbb{R}^n,$$

with

$$\bar{\mathbf{B}}_{t_0}^{t_1}(\mathbf{x}_0) := \int_{t_0}^{t_1} \mathbf{T}_{t_0}^{t}\,\nabla_0 b(\mathbf{x}_0, t)\,dt.$$

In the absence of sources and sinks ($b(\mathbf{x}_0, t) \equiv 0$), (5.10) simplifies to

$$(5.11) \qquad \mathbf{x}_0' = \bar{\mathbf{T}}_{t_0}^{t_1}(\mathbf{x}_0)\,\nabla_0 c_0(\mathbf{x}_0),$$

which leads to the following result.

Proposition 1. *Consider the time t_0 position of a perfect constrained diffusion barrier along which $\nabla_0 c_0$ is not identically zero. Then the barrier can contain no homoclinic, periodic, quasiperiodic, or almost periodic orbit.*

Proof. We use the function $V(\mathbf{x}_0) = c_0(\mathbf{x}_0)$ to note that

$$\frac{d}{ds}V(\mathbf{x}_0(s)) = \nabla_0 c_0 \cdot \mathbf{x}_0' = \left\langle \nabla_0 c_0, \bar{\mathbf{T}}_{t_0}^{t_1}\nabla_0 c_0 \right\rangle$$

along trajectories of (5.11). Since $\bar{\mathbf{T}}_{t_0}^{t_1}$ is positive definite, $V(\mathbf{x}_0(s))$ strictly increases at points where $\nabla_0 c_0$ does not vanish. This excludes the existence of any recurrent motion that contains at least one point where $\nabla_0 c_0$ does not vanish. ∎

A consequence of Proposition 1 in two dimensions is that no closed perfect constrained barriers can exist apart from closed ridges and trenches of the initial concentration field. In three dimensions, Proposition 1 implies that no two-dimensional, quasiperiodic invariant tori can arise as perfect constrained diffusion barriers, apart from toroidal ridges or trenches of the initial concentration field. Finally, for perfect constrained barriers, the DBS field defined in (5.5) simplifies to

$$(5.12) \qquad DBS_{t_1}^{t_0}(\mathbf{x}_0) = \left| \bar{\mathbf{T}}_{t_0}^{t_1}(\mathbf{x}_0)\,\nabla_0 c_0(\mathbf{x}_0) \right|.$$

In contrast to perfect barriers to diffusion, *perfect enhancers* to diffusive transport can be defined as material surfaces that pointwise maximize diffusive transport. By (5.4), the time-t_0 positions of such perfect constrained enhancers must have unit normals $\mathbf{n}_0$ satisfying

$$(5.13) \qquad\qquad \left| \left\langle \bar{\mathbf{q}}_{t_0}^{t_1}(\mathbf{x}_0), \mathbf{n}_0(\mathbf{x}_0) \right\rangle \right| = \left| \bar{\mathbf{q}}_{t_0}^{t_1}(\mathbf{x}_0) \right|.$$

Note that the norm of $\bar{\mathbf{q}}_{t_0}^{t_1}$ is not necessarily constant along such surfaces, and hence perfect transport enhancers are generally not solutions of the constrained variational problem (5.3). Instead, perfect enhancers to transport are simply surfaces that are pointwise normal to $\bar{\mathbf{q}}_{t_0}^{t_1}$, thus experiencing the locally strongest transport possible at each of their points.

In two dimensions, perfect transport enhancers are curves satisfying the ODE

$$(5.14) \qquad \mathbf{x}_0' = \boldsymbol{\Omega} \bar{\mathbf{q}}_{t_0}^{t_1}(\mathbf{x}_0) = \boldsymbol{\Omega} \left[\bar{\mathbf{T}}_{t_0}^{t_1}(\mathbf{x}_0) \boldsymbol{\nabla}_0 c_0(\mathbf{x}_0) + \bar{\mathbf{B}}_{t_0}^{t_1}(\mathbf{x}_0) \right],$$

along which $\bar{\mathbf{q}}_{t_0}^{t_1}$ has constant norm. Here we have used the notation

$$(5.15) \qquad\qquad \boldsymbol{\Omega} := \begin{pmatrix} 0 & 1 \\ -1 & 0 \end{pmatrix}$$

for planar 90-degree rotations. In the absence of sources and sinks ($b(\mathbf{x}_0, t) \equiv 0$), (5.14) simplifies to

$$(5.16) \qquad\qquad \mathbf{x}_0' = \boldsymbol{\Omega} \bar{\mathbf{T}}_{t_0}^{t_1}(\mathbf{x}_0) \boldsymbol{\nabla}_0 c_0(\mathbf{x}_0),$$

which leads to the following result.

Proposition 2. *In a two-dimensional flow, consider the time t_0 position of a closed, perfect constrained diffusion enhancer along which $\boldsymbol{\nabla}_0 c_0$ is not identically zero. Then this closed enhancer cannot be fully contained in a domain where the symmetric tensor $\boldsymbol{\Omega} \bar{\mathbf{T}}_{t_0}^{t_1}(\mathbf{x}_0) - \bar{\mathbf{T}}_{t_0}^{t_1}(\mathbf{x}_0) \boldsymbol{\Omega}$ is definite.*

Proof. As in Proposition 1, we use the function $V(\mathbf{x}_0) = c_0(\mathbf{x}_0)$ to obtain

$$\frac{d}{ds} V(\mathbf{x}_0(s)) = \boldsymbol{\nabla}_0 c_0 \cdot \mathbf{x}_0' = \left\langle \boldsymbol{\nabla}_0 c_0, \boldsymbol{\Omega} \bar{\mathbf{T}}_{t_0}^{t_1} \boldsymbol{\nabla}_0 c_0 \right\rangle$$
$$= \left\langle \boldsymbol{\nabla}_0 c_0, \left[\boldsymbol{\Omega} \bar{\mathbf{T}}_{t_0}^{t_1} - \bar{\mathbf{T}}_{t_0}^{t_1} \boldsymbol{\Omega} \right] \boldsymbol{\nabla}_0 c_0 \right\rangle$$

along trajectories of (5.16). Under the assumptions of the proposition, $V(\mathbf{x}_0(s))$ strictly increases or decreases on domains where $\boldsymbol{\Omega} \bar{\mathbf{T}}_{t_0}^{t_1}(\mathbf{x}_0) - \bar{\mathbf{T}}_{t_0}^{t_1}(\mathbf{x}_0) \boldsymbol{\Omega}$ is definite, which excludes the existence of any closed trajectory for (5.16). ∎

5.2. Constrained diffusion barriers in two-dimensional flows. The expression (5.4) is a PDE in three and more dimensions. In two dimensions, however, it is equivalent to two ODEs, as we spell out in the following result.

Theorem 5. *In two-dimensional flows, time-t_0 positions of constrained material diffusion barriers with uniform, pointwise transport density $\mathcal{T}_0$ satisfy the following necessary conditions:*

(i) *Constrained uniform transport maximizers* $\mathcal{M}_0$ *are necessarily solutions of the differential equation family*

$$(5.17) \qquad \mathbf{x}_0' = \frac{\sqrt{\left|\bar{\mathbf{q}}_{t_0}^{t_1}(\mathbf{x}_0)\right|^2 - \mathcal{T}_0^2}}{\left|\bar{\mathbf{q}}_{t_0}^{t_1}(\mathbf{x}_0)\right|^2}\bar{\mathbf{q}}_{t_0}^{t_1}(\mathbf{x}_0) \pm \frac{\mathcal{T}_0}{\left|\bar{\mathbf{q}}_{t_0}^{t_1}(\mathbf{x}_0)\right|^2}\mathbf{\Omega}\bar{\mathbf{q}}_{t_0}^{t_1}(\mathbf{x}_0), \qquad \mathcal{T}_0 > 0.$$

(ii) *If such a uniform transport maximizer* $\mathcal{M}_0$ *is a closed orbit of* (5.17) *or a homoclinic or heteroclinic orbit connecting a zero of the* $\bar{\mathbf{q}}_{t_0}^{t_1}(\mathbf{x}_0)$ *vector field to itself, then the symmetric matrix*

$$(5.18) \qquad \mathbf{L} = \int_{\mathcal{M}_0} \text{sign}\left\langle\bar{\mathbf{q}}_{t_0}^{t_1}(\mathbf{x}_0(s)), \mathbf{\Omega}\mathbf{x}_0'(s)\right\rangle \partial_{\mathbf{x}_0\mathbf{x}_0}^2 \left\langle\bar{\mathbf{q}}_{t_0}^{t_1}(\mathbf{x}_0(s)), \mathbf{\Omega}\mathbf{x}_0'(s)\right\rangle ds$$

must be negative semidefinite.

(iii) *If a uniform transport maximizer* $\mathcal{M}_0$ *satisfies*

$$\left|\bar{\mathbf{q}}_{t_0}^{t_1}(\mathbf{x}_0(s_i))\right| = \mathcal{T}_0, \;\; i = 1, 2, \quad \bar{\mathbf{q}}_{t_0}^{t_1}(\mathbf{x}_0(s_1)) \parallel \bar{\mathbf{q}}_{t_0}^{t_1}(\mathbf{x}_0(s_2)),$$

$\left|\bar{\mathbf{q}}_{t_0}^{t_1}(\mathbf{x}_0(s_i))\right| = \mathcal{T}_0$ *at its endpoints,* $\mathcal{M}_0$

$$\bar{\mathbf{q}}_{t_0}^{t_1}(\mathbf{x}_0(s_i)) \parallel \mathbf{x}_0'(s_i) \parallel \mathbf{x}_0'(s_j), \quad i, j = 1, 2, \quad i \neq j,$$

then

$$(5.19) \qquad \left\langle\mathbf{L}\mathbf{\Omega}\mathbf{x}_0', \mathbf{\Omega}\mathbf{x}_0'\right\rangle \leq 0$$

must hold along $\mathcal{M}_0$.

(iv) *Constrained uniform transport minimizers must necessarily be perfect barriers, i.e., satisfy the differential equation*

$$\mathbf{x}_0' = \bar{\mathbf{q}}_{t_0}^{t_1}(\mathbf{x}_0).$$

Proof. See Appendix C. ∎

Remark 5. The argument in the proof of (i) of Theorem 5 is not applicable to perfect diffusion barriers, as for such material lines, the leading-order term in the second variation of $\mathcal{E}(\mathcal{M}_\epsilon)$ vanishes.

In the absence of sources or sinks (i.e., for $b(\mathbf{x}_0, t) \equiv 0$ in (5.2)), (5.17) simplifies to

$$(5.20) \qquad \mathbf{x}_0' = \frac{1}{\left|\bar{\mathbf{T}}_{t_0}^{t_1}\boldsymbol{\nabla}_0 c_0\right|^2}\mathbf{A}^\pm(\mathbf{x}_0; \mathcal{T}_0)\boldsymbol{\nabla}_0 c_0(\mathbf{x}_0),$$

with the tensor $\mathbf{A}^\pm \in \mathbb{R}^2$ defined as

$$(5.21) \qquad \mathbf{A}^\pm(\mathbf{x}_0; \mathcal{T}_0) = \left(\mathcal{T}_0\mathbf{\Omega} \pm \sqrt{\left|\bar{\mathbf{T}}_{t_0}^{t_1}\boldsymbol{\nabla}_0 c_0\right|^2 - \mathcal{T}_0^2}\,\mathbf{I}\right)\bar{\mathbf{T}}_{t_0}^{t_1}.$$

In this case, the following result is helpful in the numerical identification of closed diffusion barriers as limit cycles of (5.20).

Proposition 3. *Equation* (5.20) *will have no closed (periodic or homoclinic) orbits contained entirely in spatial domains where the symmetric part of the matrix* $\mathbf{A}^{\pm} \in \mathbb{R}^2$ *is definite and* $\boldsymbol{\nabla}_0 c_0$ *is not identically zero.*

Proof. For the Lyapunov function

$$V(\mathbf{x}_0) = c_0(\mathbf{x}_0),$$

we obtain that

$$\begin{aligned}
\frac{d}{ds} V(\mathbf{x}_0(s)) &= \boldsymbol{\nabla}_0 c_0 \cdot \mathbf{x}_0' \\
&= \frac{1}{\left| \bar{\mathbf{T}}_{t_0}^{t_1} \boldsymbol{\nabla}_0 c_0 \right|^2} \left\langle \boldsymbol{\nabla}_0 c_0, \mathbf{A}^{\pm} \boldsymbol{\nabla}_0 c_0 \right\rangle.
\end{aligned}$$

Therefore, $V(\mathbf{x}_0(s))$ is strictly monotonically increasing or decreasing at least at one point of any orbit of (5.20) that lies entirely in a domain in which $\mathbf{A}^{\pm}(\mathbf{x}_0; \mathcal{T}_0)$ is definite and $\boldsymbol{\nabla}_0 c_0$ is not identically vanishing. This implies the statement of the proposition. ∎

Note that $\mathbf{A}_{t_0}^{t_1}$ is certainly definite for $\mathcal{T}_0 = 0$ at any point where $\boldsymbol{\nabla}_0 c_0$ is nonzero, and hence (5.20) has no closed orbits for $\mathcal{T}_0 = 0$, except possibly for ones along which the initial concentration gradient vanishes (curves of critical points, which is nongeneric, yet abundant in areas of constant initial concentration). This statement remains valid for small enough $\mathcal{T}_0$ on compact domains by the continuous dependence of the eigenvalues of $\mathbf{A}^{\pm}(\mathbf{x}_0; \mathcal{T}_0)$ on the parameter $\mathcal{T}_0$.

6. Particle transport barriers in stochastic velocity fields. We showed in [15] how our results on barriers to diffusive scalar transport carry over to probabilistic transport barriers to fluid particle motion with uncertainties, modeled by diffusive Itô processes. Our derivation, however, specifically exploited the incompressibility of the deterministic part of the velocity field. Here we show how similar results continue to hold for compressible Itô processes of the form

$$(6.1) \qquad d\mathbf{x}(t) = \mathbf{v}_0(\mathbf{x}(t), t)dt + \sqrt{\nu}\mathbf{B}(\mathbf{x}(t), t)d\mathbf{W}(t).$$

Here $\mathbf{x}(t) \in \mathbb{R}^n$ is the random position vector of a particle at time t; $\mathbf{v}_0(\mathbf{x}, t)$ denotes the deterministic, generally compressible drift component in the velocity of the particle motion and $\mathbf{W}(t)$ in an m-dimensional Wiener process with diffusion matrix $\sqrt{\nu}\mathbf{B}(\mathbf{x}, t) \in \mathbb{R}^{n \times m}$. Here the dimensionless, nonsingular diffusion structure matrix $\mathbf{B}$ is $\mathcal{O}(1)$ with respect to the small parameter $\nu > 0$.

We let $p(\mathbf{x}, t; \mathbf{x}_0, t_0)$ denote the probability density function (PDF) for the current particle position $\mathbf{x}(t)$ with initial condition $\mathbf{x}_0(t_0) = \mathbf{x}_0$. This PDF satisfies the classic Fokker–Planck equation (see, e.g., Risken [29])

$$(6.2) \qquad p_t + \boldsymbol{\nabla} \cdot (p\mathbf{v}_0) = \nu \tfrac{1}{2} \boldsymbol{\nabla} \cdot \left[\boldsymbol{\nabla} \cdot \left(\mathbf{B}\mathbf{B}^{\top} p \right) \right],$$

or, alternatively,

$$(6.3) \qquad p_t + \boldsymbol{\nabla} \cdot (p\tilde{\mathbf{v}}_0) = \nu \boldsymbol{\nabla} \cdot \left(\tfrac{1}{2} \mathbf{B}\mathbf{B}^{\top} \boldsymbol{\nabla} p \right), \quad \tilde{\mathbf{v}}_0 = \mathbf{v}_0 - \tfrac{\nu}{2} \boldsymbol{\nabla} \cdot \left(\mathbf{B}\mathbf{B}^{\top} \right).$$

This latter equation is of the advection-diffusion form (2.3) if we select

$$(6.4) \qquad c := \frac{p}{\rho}, \quad \mathbf{D} := \tfrac{1}{2}\mathbf{B}\mathbf{B}^{\top}, \quad \mathbf{w} := \tilde{\mathbf{v}}_0 = \mathbf{v}_0 - \nu \boldsymbol{\nabla} \cdot \mathbf{D}, \quad k(t) = f(\mathbf{x}, t) \equiv 0.$$

Consequently, the Fokker–Planck equation (6.3) is equivalent to the advection-diffusion equation (2.1) with the velocity field

$$(6.5) \qquad \mathbf{v} := \mathbf{w} - \frac{\nu}{\rho}\mathbf{D}\boldsymbol{\nabla}\rho = \mathbf{v}_0 - \nu\boldsymbol{\nabla} \cdot \mathbf{D} - \frac{\nu}{\rho}\mathbf{D}\boldsymbol{\nabla}\rho.$$

Since the equation of continuity,

$$(6.6) \qquad \partial_t \rho + \boldsymbol{\nabla} \cdot (\rho\mathbf{v}) = 0,$$

must hold for the velocity field $\mathbf{v}$ for our formulation to apply, substitution of the definition of $\mathbf{v}$ from (6.5) into (6.6) gives

$$\partial_t \rho + \boldsymbol{\nabla} \cdot \left[\rho \left(\mathbf{v}_0 - \frac{\nu}{\rho}\mathbf{D}\boldsymbol{\nabla}\rho - \nu\boldsymbol{\nabla} \cdot \mathbf{D} \right) \right] = 0$$

or, equivalently,

$$(6.7) \qquad \partial_t \rho + \boldsymbol{\nabla} \cdot (\rho\mathbf{v}_0) = \nu\boldsymbol{\nabla} \cdot (\boldsymbol{\nabla} \cdot (\mathbf{D}\rho)),$$

which is the same PDE (6.3) that the probability density p satisfies.

With the above choice of $\mathbf{v}$ and ρ in (6.5) and (6.7), all results in the earlier sections on material diffusion extremizers in compressible flows carry over to material diffusion barriers of the density-weighted PDF $c = p/\rho$ with respect to the velocity field $\mathbf{v}$ in (6.5) if we redefine the transport tensor $\mathbf{T}_{t_0}^t(\mathbf{x}_0)$ as

$$(6.8) \qquad \mathbf{T}_{t_0}^t(\mathbf{x}_0) := \tfrac{1}{2}\rho_0(\mathbf{x}_0) \left[\boldsymbol{\nabla}_0\mathbf{F}_{t_0}^t(\mathbf{x}_0) \right]^{-1} \mathbf{B}(\mathbf{F}_{t_0}^t(\mathbf{x}_0), t)\mathbf{B}^{\top}(\mathbf{F}_{t_0}^t(\mathbf{x}_0), t) \left[\boldsymbol{\nabla}_0\mathbf{F}_{t_0}^t(\mathbf{x}_0) \right]^{-T}.$$

Furthermore, let us denote the initial PDF by $p_0(\mathbf{x}) := p(\mathbf{x}, t_0; \mathbf{x}_0, t_0)$ and assume the initial carrier fluid density $\rho_0(\mathbf{x})$ as given. Then, with the help of the vector field (cf. (5.2))

$$(6.9) \qquad \bar{\mathbf{q}}_{t_0}^{t_1}(\mathbf{x}_0) = \int_{t_0}^{t_1} \left[\mathbf{T}_{t_0}^t(\mathbf{x}_0)\boldsymbol{\nabla}_0 \frac{p_0(\mathbf{x}_0)}{\rho_0(\mathbf{x}_0)} \right] dt,$$

we collect the related results in the following theorem.

Theorem 6. (i) *Unconstrained, uniform barriers of transport for the mass-based PDF, p/ρ, of particle positions satisfy Theorems 2–5 with the transport tensor field $\mathbf{T}_{t_0}^t(\mathbf{x}_0)$ defined as in (6.8).*

(ii) *Constrained, uniform barriers of transport for the mass-based PDF, p/ρ, satisfy Theorems 4–3 with the transport vector field $\bar{\mathbf{q}}_{t_0}^{t_1}(\mathbf{x}_0)$ defined as in (6.9).*

Proof. Indeed, for the case of an unspecified initial density $c_0(\mathbf{x})$, we obtain the normalized total transport of $\mu(\mathbf{x}, t)$ in the form (cf. (4.2))

$$(6.10) \qquad \widetilde{\Sigma}_{t_0}^{t_1}(\mathcal{M}_0) = \frac{\Sigma_{t_0}^{t_1}(\mathcal{M}_0)}{\nu K (t_1 - t_0) A_0(\mathcal{M}_0)} = \frac{\int_{\mathcal{M}_0} \left\langle \mathbf{n}_0, \bar{\mathbf{T}}_{t_0}^{t_1} \mathbf{n}_0 \right\rangle dA_0}{\int_{\mathcal{M}_0} dA_0} + o(\nu^\alpha), \quad \nu \in (0, 1],$$

with the transport tensor (6.8), where $\mathbf{F}_{t_0}^t(\mathbf{x}_0)$ is the flow map associated with the velocity field $\mathbf{v}_0(\mathbf{x}, t)$ and $\rho_0(\mathbf{x}_0)$ is the initial density field of the carrier fluid, serving as initial condition for the density evolution equation (6.7). The formulas (6.8)–(6.10) follow because the flow map of the full velocity field $\mathbf{v}$ defined in (6.5) is at least $\mathcal{O}(\nu)$ C^0-close to the flow map $\mathbf{F}_{t_0}^t(\mathbf{x}_0)$ of $\mathbf{v}_0(\mathbf{x}, t)$ over the finite time interval $[t_0, t_1]$. As a consequence, only the leading-order term, $\mathbf{F}_{t_0}^t(\mathbf{x}_0)$, of the flow map generated by (6.5) appears in the transport tensor (6.8). Higher-order corrections to the full flow map can be subsumed into the $o(\nu^\alpha)$ term in (6.10). With this observation, statements (i) and (ii) can be deduced in the same fashion as Theorems 2–3 and Theorems 4–5. ∎

Based on Theorem 6, the arguments leading to the diffusion barrier strength indicator in (4.8)–(5.5) continue to apply, with the DBS field simplified to

$$DBS_{t_0}^{t_1}(\mathbf{x}_0) = \left| \bar{\mathbf{T}}_{t_0}^{t_1}(\mathbf{x}_0) \nabla_0 \frac{p_0(\mathbf{x})}{\rho_0(\mathbf{x})} \right|.$$

7. Examples. In this section, we illustrate our results on advection-diffusion problems with explicitly known solutions. These problems are defined by simple velocity fields, which in turn generate simple diffusion barrier and enhancer geometries. This simplicity enables a detailed quantitative validation of our theory.

We consider solutions of the planar vorticity-transport equation

$$(7.1) \qquad\qquad\qquad\qquad \partial_t \omega + \nabla \omega \cdot \mathbf{v} = \nu \Delta \omega$$

with kinematic viscosity ν for a two-dimensional, incompressible velocity field $\mathbf{v}(\mathbf{x}, t)$ defined over $\mathbf{x} = (x, y) \in U = \mathbb{R}^2$. In this two-dimensional setting, the only nonzero component of the curl of $\mathbf{v}$ is normal to the plane and is given by the scalar vorticity

$$(7.2) \qquad\qquad \omega(\mathbf{x}, t) = [\nabla \times \mathbf{v}(\mathbf{x}, t)]_z = \partial_x v_2(x, y, t) - \partial_y v_1(x, y, t).$$

Formula (7.2) shows that (7.1) is a nonlinear PDE for an unknown velocity field $\mathbf{v}$. At the same time, once the velocity field $\mathbf{v}$ is known, (7.1) becomes a linear advection-diffusion equation of the form (2.1) for the scalar vorticity field $\omega(\mathbf{x}, t)$ with $\rho(\mathbf{x}, t) \equiv 1$, $\mathbf{D}(\mathbf{x}, t) \equiv \mathbf{I}$, and $k(t) = f(\mathbf{x}, t) \equiv 0$. Importantly, however, the only admissible initial condition for the advection-diffusion formulation of (7.1) at a time $t = t_0$ is the one consistent with the initial velocity field:

$$(7.3) \qquad\qquad\qquad\qquad \omega_0(\mathbf{x}) = [\nabla \times \mathbf{v}_0(\mathbf{x})]_z.$$

Under this initial condition, the solution of the advection-diffusion equation (7.1) will coincide with $[\nabla \times \mathbf{v}(\mathbf{x}, t)]_z$ for all times. Due to the inevitable constraint (7.3), our theory of constrained diffusion barriers for two-dimensional flows (cf. section 5.2) will be applicable here to explore diffusive transport in (7.1).
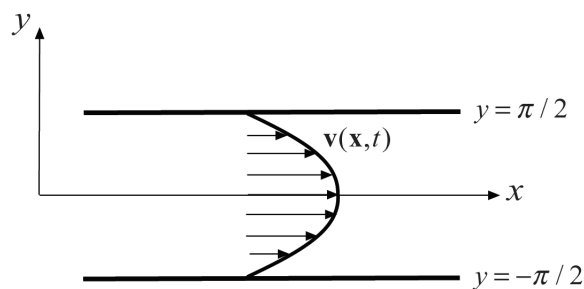
Figure 7.1. *Unsteady, horizontal jet with a jet core at $y = 0$.*

7.1. Two-dimensional channel flow. An unsteady solution of the two-dimensional, un-forced Navier–Stokes equations is given by the decaying channel flow

$$(7.4) \qquad \mathbf{v}(\mathbf{x}, t) = e^{-\nu t} \begin{pmatrix} a \cos y \\ 0 \end{pmatrix},$$

whose vorticity field is

$$\omega(\mathbf{x}, t) = a e^{-\nu t} \sin y.$$

The simplest member of a more general Navier–Stokes solution family (see, e.g., Majda and Bertozzi [24]), the velocity field (7.4) describes a decaying horizontal shear-jet between two no-slip boundaries at $y = \pm \frac{\pi}{2}$ (see Figure 7.1).

The jet core is given by the horizontal line $y = 0$. The constant $a \in \mathbb{R}^+$ governs the strength of shear within the jet. If we define the variable x to be spatially periodic, the flow becomes a model of a perfectly circular vortical flow in an annulus with no-slip walls.

All horizontal lines are invariant material lines in (7.4). Of these invariant lines, the jet core at $y = 0$ is the most often noted barrier to the diffusion of vorticity, keeping positive and negative vorticity values apart for all times. Indeed, for large values of a, the norm of the vorticity gradient

$$\nabla \omega(\mathbf{x}, t) = e^{-\nu t} \begin{pmatrix} 0 \\ a \cos y \end{pmatrix}$$

maintains its global maximum along the jet core for all times. The upper and lower channel boundaries at $y = \pm \pi/2$ technically also block the diffusion of vorticity into the wall, but vorticity tapers off to zero anyway as one approaches these boundaries in the vertical direction.

As the initial distribution of $\omega(\mathbf{x}, t)$ is constrained by the velocity field, our theory of constrained diffusion barriers is applicable to barriers to the transport of vorticity. To see the predictions of this theory, we first note that the flow map $\mathbf{F}_{t_0}^{t}(\mathbf{x}_0)$ in this example is

$$\mathbf{F}_{t_0}^{t}(\mathbf{x}_0) = \begin{pmatrix} x_0 - \dfrac{a}{\nu}\left(e^{-\nu t} - e^{-\nu t_0}\right) \cos y_0 \\ \\ y_0 \end{pmatrix},$$

which gives

$$\boldsymbol{\nabla}_0 \left[\omega \left(\mathbf{F}_{t_0}^t \left(\mathbf{x}_0 \right), t \right) \right] = a e^{-\nu t} \begin{pmatrix} 0 \\ \cos y_0 \end{pmatrix},$$

$$\mathbf{T}_{t_0}^t (\mathbf{x}_0) = \begin{pmatrix} 1 + \dfrac{a^2}{\nu^2} \left(e^{-\nu t} - e^{-\nu t_0} \right)^2 \sin^2 y_0 & -\dfrac{a}{\nu} \left(e^{-\nu t} - e^{-\nu t_0} \right) \sin y_0 \\ -\dfrac{a}{\nu} \left(e^{-\nu t} - e^{-\nu t_0} \right) \sin y_0 & 1 \end{pmatrix}.$$

Therefore,

$$\bar{\mathbf{q}}_{t_0}^{t_1} (\mathbf{x}_0) = \frac{1}{t_1 - t_0} \int_{t_0}^{t_1} \mathbf{T}_{t_0}^t (\mathbf{x}_0) \boldsymbol{\nabla}_0 \left[\omega \left(\mathbf{F}_{t_0}^t \left(\mathbf{x}_0 \right), t \right) \right] dt$$

$$= \frac{1}{2\nu \left(t_1 - t_0 \right)} \begin{pmatrix} A \sin 2y_0 \\ B \cos y_0 \end{pmatrix},$$

where

$$A = \frac{a^2}{\nu} \sin 2y_0 \left[\frac{1}{2} e^{-2\nu t_1} + \frac{1}{2} e^{-2\nu t_0} - e^{-\nu(t_1 + t_0)} \right], \qquad B = a \left(e^{-\nu t_0} - e^{-\nu t_1} \right).$$

Consequently, the ODE family describing the time t_0 position of uniform constrained barriers is given by

$$(7.5) \quad \mathbf{x}_0' = \frac{1}{2\nu \left(t_1 - t_0 \right)} \left\{ \frac{\sqrt{\left| \bar{\mathbf{q}}_{t_0}^{t_1} (\mathbf{x}_0) \right|^2 - \mathcal{T}_0^2}}{\left| \bar{\mathbf{q}}_{t_0}^{t_1} (\mathbf{x}_0) \right|^2} \begin{pmatrix} A \sin 2y_0 \\ B \cos y_0 \end{pmatrix} + \frac{\mathcal{T}_0}{\left| \bar{\mathbf{q}}_{t_0}^{t_1} (\mathbf{x}_0) \right|^2} \begin{pmatrix} B \cos y_0 \\ -A \sin 2y_0 \end{pmatrix} \right\}$$

for some value of the transport density $\mathcal{T}_0 \in \mathbb{R}$. For the choice

$$(7.6) \qquad \mathcal{T}_0 = \left. \left| \bar{\mathbf{q}}_{t_0}^{t_1} (\mathbf{x}_0) \right| \right|_{y_0=0} = \frac{B}{2\nu \left(t_1 - t_0 \right)},$$

the ODE (7.5) becomes

$$(7.7) \qquad \left. \mathbf{x}_0' \right|_{y_0=0} = \frac{B}{2\nu \left(t_1 - t_0 \right)} \begin{pmatrix} B \\ 0 \end{pmatrix} \parallel \left. \boldsymbol{\Omega} \bar{\mathbf{q}}_{t_0}^{t_1} (\mathbf{x}_0) \right|_{y_0=0}.$$

Therefore, $y_0 = 0$ is an invariant line for (7.5) for the parameter value $\mathcal{T}_0$ selected as in (7.6). Consequently, the jet core at $y_0 = 0$ is a uniform, constrained barrier to vorticity diffusion along which the pointwise diffusive transport of vorticity is equal to (7.5). As noted earlier, a barrier (as a stationary surface of the transport functional) is not necessarily a minimizer of transport. Indeed, any other horizontal material curve admits a strictly lower transport density than the jet core.

In contrast, choosing the constant

$$\mathcal{T}_0 = 0$$

in (7.5) gives the ODE

$$\mathbf{x}_0' = \frac{1}{2\nu a\,(t_1 - t_0)\,\left|\bar{\mathbf{q}}_{t_0}^{t_1}\,(\mathbf{x}_0)\right|} \begin{pmatrix} A\sin 2y_0 \\ B\cos y_0 \end{pmatrix},$$

for which $y_0 = \pm\pi/2$ are invariant lines. Along those invariant lines, we have

$$\mathbf{x}_0'\big|_{y_0=\pm\pi/2} \; \parallel \; \bar{\mathbf{q}}_{t_0}^{t_1}\,(\mathbf{x}_0)\big|_{y_0=\pm\pi/2}.$$

Therefore, the channel walls at $y_0 = \pm\pi/2$ are uniform, constrained minimizers to vorticity diffusion along which the pointwise diffusive transport of vorticity is equal to zero. In particular, the channel walls are perfect constrained barriers to diffusive transport.

To evaluate the second necessary condition we need to check the definiteness of the matrix

$$\mathbf{L} = \int_{\mathcal{M}_0} \operatorname{sign}\left\langle \bar{\mathbf{q}}_{t_0}^{t_1}\,(\mathbf{x}_0(s))\,,\mathbf{\Omega}\mathbf{x}_0'(s)\right\rangle \partial_{\mathbf{x}_0\mathbf{x}_0}^2 \left\langle \bar{\mathbf{q}}_{t_0}^{t_1}\,(\mathbf{x}_0(s))\,,\mathbf{\Omega}\mathbf{x}_0'(s)\right\rangle ds.$$

Note that

$$\begin{aligned}
\partial_{\mathbf{x}_0\mathbf{x}_0}^2 \left\langle \bar{\mathbf{q}}_{t_0}^{t_1}\,(\mathbf{x}_0(s))\,,\mathbf{\Omega}\mathbf{x}_0'(s)\right\rangle |_{y_0=0} &= \partial_{\mathbf{x}_0\mathbf{x}_0}^2 \left[\frac{1}{2\nu\,(t_1-t_0)} \begin{pmatrix} A\sin 2y_0 \\ B\cos y_0 \end{pmatrix}\right]|_{y_0=0} \cdot \mathbf{\Omega}\mathbf{x}_0'(s)|_{y_0=0} \\
&= \partial_{\mathbf{x}_0\mathbf{x}_0}^2 \left[\frac{1}{2\nu\,(t_1-t_0)} \begin{pmatrix} A\sin 2y_0 \\ B\cos y_0 \end{pmatrix} \cdot \frac{B}{2\nu\,(t_1-t_0)} \begin{pmatrix} 0 \\ -B \end{pmatrix}\right]|_{y_0=0} \\
&= \frac{B^2}{4\nu^2\,(t_1-t_0)^2} \partial_{\mathbf{x}_0\mathbf{x}_0}^2 \left[\begin{pmatrix} A\sin 2y_0 \\ B\cos y_0 \end{pmatrix} \cdot \begin{pmatrix} 0 \\ -1 \end{pmatrix}\right]|_{y_0=0} \\
&= \frac{-B^3}{4\nu^2\,(t_1-t_0)^2} \partial_{\mathbf{x}_0\mathbf{x}_0}^2 \left[\cos y_0\right]|_{y_0=0} \\
&= \frac{-B^3}{4\nu^2\,(t_1-t_0)^2} \begin{pmatrix} 0 & 0 \\ 0 & -\cos y_0 \end{pmatrix}|_{y_0=0} \\
&= \frac{B^3}{4\nu^2\,(t_1-t_0)^2} \begin{pmatrix} 0 & 0 \\ 0 & 1 \end{pmatrix},
\end{aligned}$$

and

$$\operatorname{sign}\left\langle \bar{\mathbf{q}}_{t_0}^{t_1}\,(\mathbf{x}_0(s))\,,\mathbf{\Omega}\mathbf{x}_0'(s)\right\rangle |_{y_0=0} = \frac{-B^3}{4\nu^2\,(t_1-t_0)^2} \left[\cos y_0\right]\big|_{y_0=0} = -1.$$

As a consequence, we have

$$\begin{aligned}
\mathbf{L} &= \int_{\mathcal{M}_0} \operatorname{sign}\left\langle \bar{\mathbf{q}}_{t_0}^{t_1}\,(\mathbf{x}_0(s))\,,\mathbf{\Omega}\mathbf{x}_0'(s)\right\rangle \partial_{\mathbf{x}_0\mathbf{x}_0}^2 \left\langle \bar{\mathbf{q}}_{t_0}^{t_1}\,(\mathbf{x}_0(s))\,,\mathbf{\Omega}\mathbf{x}_0'(s)\right\rangle ds \\
&= -\frac{B^6 \operatorname{length}(\mathcal{M}_0)}{16\nu^4\,(t_1-t_0)^4} \begin{pmatrix} 0 & 0 \\ 0 & 1 \end{pmatrix},
\end{aligned}$$

implying

$$\left\langle \mathbf{L}\mathbf{\Omega}\mathbf{x}_0',\mathbf{\Omega}\mathbf{x}_0'\right\rangle \leq 0$$

satisfying the necessary condition (5.19) for a maximizer.

In summary, our theory correctly identifies the walls and the jet core as noteworthy features of this channel flow. While these features are all considered as inhibitors of transport in informal descriptions of jet-type flows, our approach reveals that in strict mathematical terms, only the walls act as diffusion minimizers. The jet core, in contrast, is a diffusion maximizer with respect to any localized perturbation and with respect to parallel translations.

7.2. Spatially periodic recirculation cells. A spatially periodic, unsteady solution of the two-dimensional Navier–Stokes equations is given by (cf. Majda and Bertozzi [24])

$$(7.8) \qquad \mathbf{v}(\mathbf{x},t) = a\mathrm{e}^{-4\pi^2\nu t} \begin{pmatrix} \sin(2\pi x)\sin(2\pi y) \\ \cos(2\pi x)\cos(2\pi y) \end{pmatrix},$$

whose vorticity field and Jacobian are given by

$$\omega(\mathbf{x},t) = -4a\pi\mathrm{e}^{-4\pi^2\nu t}\sin(2\pi x)\cos(2\pi y),$$

$$(7.9) \qquad \boldsymbol{\nabla}\mathbf{v}(\mathbf{x},t) = 2\pi a\mathrm{e}^{-4\pi^2\nu t} \begin{pmatrix} \cos(2\pi x)\sin(2\pi y) & \sin(2\pi x)\cos(2\pi y) \\ -\sin(2\pi x)\cos(2\pi y) & -\cos(2\pi x)\sin(2\pi y) \end{pmatrix}.$$

The vorticity field ω satisfies the advection-diffusion equation (7.1) with viscosity ν and a real parameter a that controls its overall strength.

The vorticity gradient is

$$\boldsymbol{\nabla}\omega\,(\mathbf{x},t) = -8a\pi^2\mathrm{e}^{-4\pi^2\nu t} \begin{pmatrix} \cos(2\pi x)\cos(2\pi y) \\ -\sin(2\pi x)\sin(2\pi y) \end{pmatrix} = -8a\pi^2\boldsymbol{\Omega}\mathbf{v}(\mathbf{x},t),$$

whose squared norm satisfies

$$\frac{|\boldsymbol{\nabla}\omega\,(\mathbf{x},t)|^2}{\left(8\pi^2\mathrm{e}^{-4\pi^2\nu t}\right)^2} = a^2\left[\cos^2(2\pi x)\cos^2(2\pi y) + \sin^2(2\pi x)\sin^2(2\pi y)\right] \le a^2.$$

The flow has horizontal and vertical heteroclinic orbits connecting the array of saddle-type fixed points at $(x,y) = (\frac{j}{4},\frac{k}{4})$ for arbitrary integers j and k. This heteroclinic network surrounds an array of vortical recirculation regions. Even though the velocity field is unsteady, its streamline geometry consists of steady material lines (cf. Figure 7.2). Only the value of the vorticity changes in time by the same factor along these material lines, just as in our previous example.

The main observed features in the diffusive transport of vorticity in this flow are the cell boundaries formed by the heteroclinic orbits. Along these orbits, $|\boldsymbol{\nabla}\omega\,(\mathbf{x},t)|^2$ admits maximum ridges that decay slowly in time by a uniform factor. The ridges contain global minima with $|\boldsymbol{\nabla}\omega|^2 = 0$ at the hyperbolic equilibria and global maxima with $|\boldsymbol{\nabla}\omega|^2 = a^2(8\pi^2\mathrm{e}^{-4\pi^2\nu t})^2$ halfway between them. Inside the cells, $|\boldsymbol{\nabla}\omega|^2$ decays away from the ridge boundaries and reaches the global minimum $|\boldsymbol{\nabla}\omega|^2 = 0$ again at the elliptic equilibria. All closed, periodic streamlines in the vortical region are also perceived as features hindering the spread of high vorticity from the centers of the vortical regions.
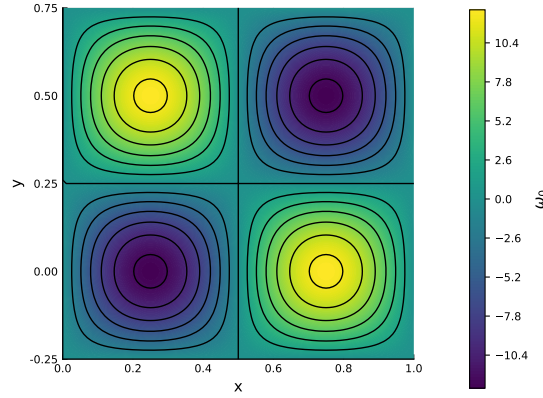
Figure 7.2. *Unsteady vortex array with $a = 1$ at time $t = 0$.*

We now examine how our theory of constrained diffusion extremizers bears on the vorticity field features identified above from observations. Along, say, the $y = 0.25$ horizontal heteroclinic streamline, the velocity Jacobian (7.9) becomes

$$\boldsymbol{\nabla}\mathbf{v}((x, 0.25), t) = 2\pi a \cos(2\pi x)\mathrm{e}^{-4\pi^2 \nu t}\begin{pmatrix} 1 & 0 \\ 0 & -1 \end{pmatrix},$$

implying

$$\left[\boldsymbol{\nabla}_0 \mathbf{F}_{t_0}^t((x_0, 0.25))\right]^{-1} =$$
$$\begin{pmatrix} \exp\left(-\int_{t_0}^t 2\pi a \cos(2\pi x(s))\mathrm{e}^{-4\pi^2 \nu s}ds\right) & 0 \\ 0 & \exp\left(\int_{t_0}^t 2\pi a \cos(2\pi x(s))\mathrm{e}^{-4\pi^2 \nu s}ds\right) \end{pmatrix},$$
$$\boldsymbol{\nabla}\omega\left(\mathbf{F}_{t_0}^t((x_0, 0.25)), t\right) = 8a\pi^2 \sin(2\pi x(t))\mathrm{e}^{-4\pi^2 \nu t}\begin{pmatrix} 0 \\ 1 \end{pmatrix}.$$

This gives

$$\left[\boldsymbol{\nabla}_0 \mathbf{F}_{t_0}^t(\mathbf{x}_0)\right]^{-1}\boldsymbol{\nabla}\omega\left(\mathbf{F}_{t_0}^t(\mathbf{x}_0), t\right) \parallel \begin{pmatrix} 0 \\ 1 \end{pmatrix},$$

and hence, for any $t_1 > t_0$ and for any initial point $\mathbf{x}_0 = (x_0, 0.25)$, we have (cf. Remark 4)

$$\bar{\mathbf{q}}_{t_0}^{t_1}(\mathbf{x}_0) = \frac{1}{t_1 - t_0}\int_{t_0}^{t_1}\left[\boldsymbol{\nabla}_0 \mathbf{F}_{t_0}^t(\mathbf{x}_0)\right]^{-1}\boldsymbol{\nabla}\omega\left(\mathbf{F}_{t_0}^t(\mathbf{x}_0), t\right)dt \parallel \begin{pmatrix} 0 \\ 1 \end{pmatrix}.$$

We conclude that $y = 0.25$ horizontal heteroclinic streamline with unit normal $\mathbf{n}_0(\mathbf{x}_0) = (0, 1)$ is a perfect transport enhancer in the sense of formula (5.13). An identical conclusion holds for all other heteroclinic connections.

In contrast, along closed, vortical streamlines, we find the integrand of $\bar{\mathbf{q}}_{t_0}^{t_1}(\mathbf{x}_0)$ to align with these streamlines due to the shearing effect of the inverse flow map $\left[\boldsymbol{\nabla}_0 \mathbf{F}_{t_0}^t(\mathbf{x}_0)\right]^{-1}$ on
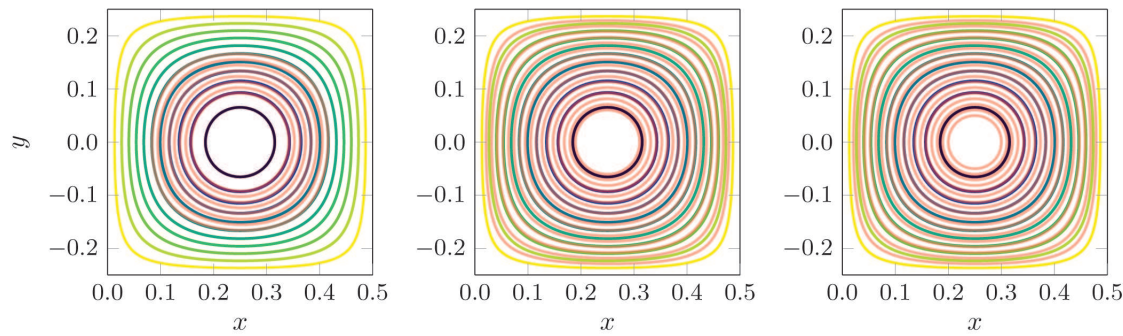
Figure 7.3. *Closed material vorticity transport barriers (in light red) in the lower-left recirculation cell of Figure 7.2 for integration times $T = 3$, $T = 13$, and $T = 23$ (from left to right), on top of vorticity level sets (yellow-green-blue).*

the streamline-normal vorticity gradient $\boldsymbol{\nabla}\omega\left(\mathbf{F}_{t_0}^t\left(\mathbf{x}_0\right),t\right)$. *This implies that in the $t_1 \to \infty$ limit, all closed streamlines become asymptotically perfect transport barriers, with their normals asymptotically aligning with $\bar{\mathbf{q}}_{t_0}^{t_1}(\mathbf{x}_0)$ at the same rate at all of their points.*

For finite times, the exact closed transport barriers in this flow can be identified numerically by computing the ODEs appearing in Theorem 5 for the velocity field (5). For this computation, we set $a = 1$ and $\nu = 0.001$. The results in Figure 7.3 show a close match between an increasing number of detected barriers and vorticity level sets as the integration time is extended from $T = 3$ (left) via $T = 13$ (middle) up to $T = 23$ (right).

8. Application to transport-barrier detection in ocean-surface dynamics.
We now illustrate our results on two different ocean surface velocity data sets. The first one is HYCOM, a data-assimilating hybrid ocean model, whose ocean-surface velocity output is generally not divergence-free and hence represents a compressible two-dimensional flow. The second data set is a two-dimensional unsteady velocity field obtained from AVISO satellite altimetry measurements under the geostrophic approximation. This data set is currently distributed by the Copernicus Marine and Environment Monitoring Service. Due to the geostrophic approximation, this velocity field is constructed as divergence-free.

To apply the two-dimensional unconstrained diffusion barrier results of section 4.2 to the HYCOM data set, we use the coherent-structure and diffusion-barrier computation package CoherentStructures.jl written in Julia [3]. This package computes trajectories of the direction field (4.9), as described in [18]. To apply the two-dimensional constrained diffusion barriers results of section 5.2, we use the ODE integration codes provided by the DifferentialEquations.jl package of [28].

An alternative implementation of our constrained and unconstrained diffusion barrier results for two-dimensional data sets is available in the open source MATLAB GUI BarrierTool, which utilizes the results of [31] to compute diffusion barriers as null-geodesics of appropriate tensor fields.
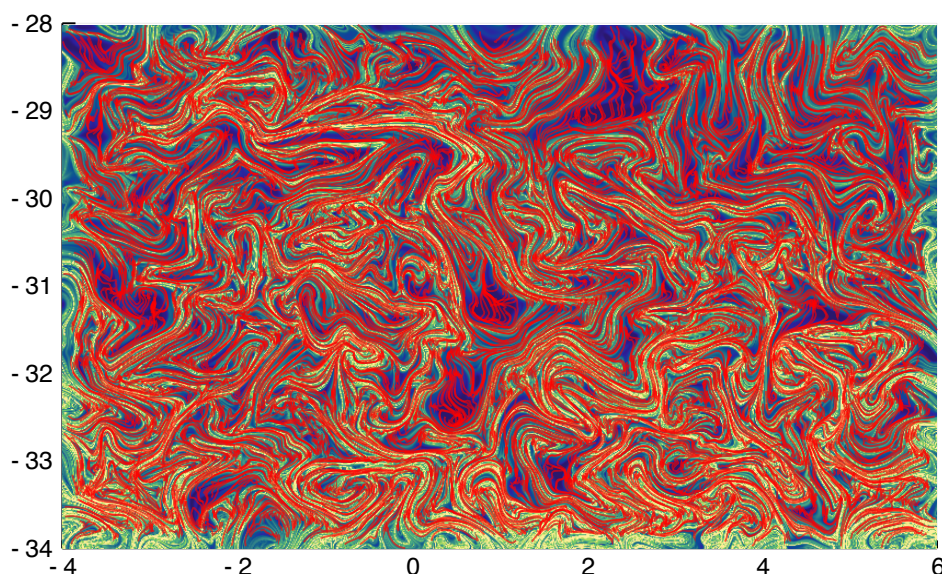
Figure 8.1. *Open transport barriers in the HYCOM ocean surface data set. Shown in the background is the DBS field (with tails cut for visualization purposes). Overlaid are short integral curve segments of the $\boldsymbol{\eta}_{\mathcal{T}_0}^+$ field (equation (4.9)) for $\mathcal{T}_0 = 1$. Other values of $\mathcal{T}_0$ produce similar results.*

**8.1. Unconstrained transport barriers in the compressible HYCOM velocity data set.** We use ocean surface velocity data from December 15, 2013, to January 14, 2014, i.e., 30 days, taken from the Agulhas leakage area at the southern tip of Africa. The choice of the $[t_0, t_1]$ time interval is for illustration; different choices of the time interval yield different results. This is because, unlike the simple velocity fields treated in the examples of section 7, the HYCOM velocity field defines a general, finite-time nonautonomous dynamical system for the fluid motion, with no recurrent time-dependence. The time interval $[t_0, t_1]$ is part of the definition of this dynamical system. Changing this interval changes the dynamical system and generally results in different transport barriers and enhancers.

In Figure 8.1, we show the diagnostic DBS field (4.8), whose features align, as expected, remarkably close with the unconstrained, uniform transport barriers extracted as trajectories of the $\boldsymbol{\eta}_{\mathcal{T}_0}^+$ field (4.9) for $\mathcal{T}_0 = 1$.

As a second step, we now verify if these material curves (obtained from purely advective calculations) indeed act as observed transport barriers for a diffusive scalar field. To this end, we solve the advection-diffusion equation (2.1), with $k(t) = f(\mathbf{x}, t) \equiv 0$ and $\mathbf{D}(\mathbf{x}, t) \equiv \mathbf{I}$, in Lagrangian coordinates for the initial concentration shown in Figure 8.2 (left). The final density obtained from this computation is then shown in Figure 8.2 (right), with the same uniform transport barriers overlaid as in Figure 8.1. Note how the predicted barriers indeed capture detailed features in the evolving concentration field.

8.2. Constrained diffusion barriers in the AVISO velocity data. We now illustrate our results on two-dimensional unsteady velocity data obtained from AVISO satellite altimetry
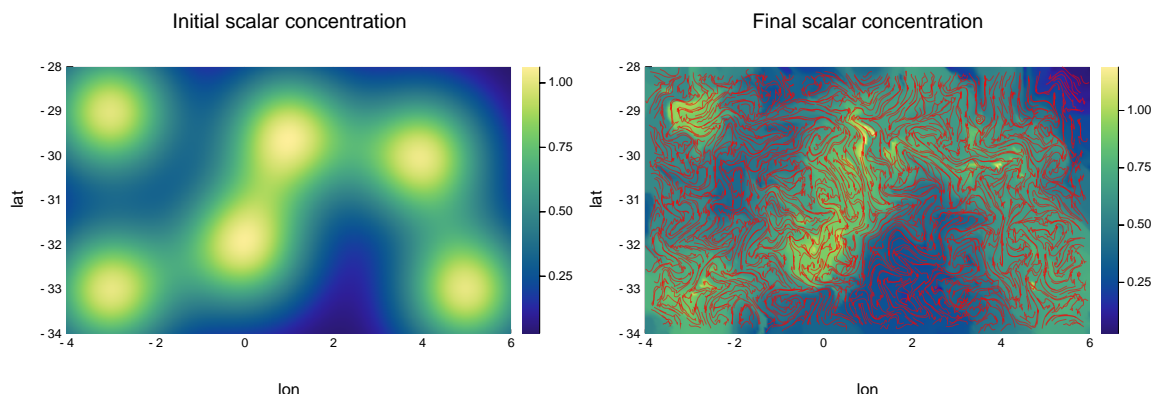
Figure 8.2. *Transport barriers in the HYCOM ocean surface data set. The scalar field corresponds to the initial (left) and final (right) scalar density, evolved under the advection-diffusion equation* (2.1) *in Lagrangian coordinates. The final scalar concentration field is shown with short integral curve segments of the $\boldsymbol{\eta}_{\mathcal{T}_0}^+$ field (equation* (4.9)*) overlaid for a small value $\mathcal{T}_0 = 1$ of the nondimensionalized, uniform transport density.*

measurements. The domain of the dataset is the Agulhas leakage in the Southern Ocean. Under the assumption of a geostrophic flow, the sea surface height h serves as a streamfunction for the surface velocity field. In longitude-latitude coordinates (φ, θ), particle trajectories are then solutions of the system

$$(8.1) \qquad \dot{\varphi} = -\frac{g}{R^2 f(\theta) \cos \theta} \partial_\theta h(\varphi, \theta, t), \qquad \dot{\theta} = \frac{g}{R^2 f(\theta) \cos \theta} \partial_\varphi h(\varphi, \theta, t),$$

where g is the constant of gravity, R is the mean radius of the Earth, and $f(\theta) \coloneqq 2\Omega \sin \theta$ is the Coriolis parameter with Ω denoting the mean angular velocity of the Earth. The computational domain is chosen as in several other previous studies (see, e.g., [14, 16, 15]), with integration time T equal to 90 days.

In this two-dimensional flow, we wish to determine material transport barriers for the vorticity $\omega(\mathbf{x}, t)$, i.e., the single nonzero component of $\nabla \times \mathbf{v}$ normal to the plane of the flow (equation (8.1)). Following Remark 4, we use the exact transport vector field $\bar{\mathbf{q}}_{t_0}^{t_1}$, (5.8). For closed-orbit detection, we employ a numerical scheme described in [18], which builds on [16], with

1. an index-theory-based preselection of elliptic-type subdomains;
2. placement of Poincaré sections in regions with an appropriate index;
3. launch of integral curves from seed points, solving for the transport parameter which yields a closed orbit at the respective seed point.

The closed material vorticity transport barriers obtained from this procedure are shown in Figure 8.3, on top of the initial (left) and final (right) vorticity fields in Lagrangian coordinates. We note that closed diffusion barriers arise around all four vortical regions identified by previous studies (see, e.g., [14, 16, 13, 31, 15]) as materially coherent. The closed region boundaries here are optimized to be extremizers of the vorticity transport, as opposed to outermost coherent material curves.
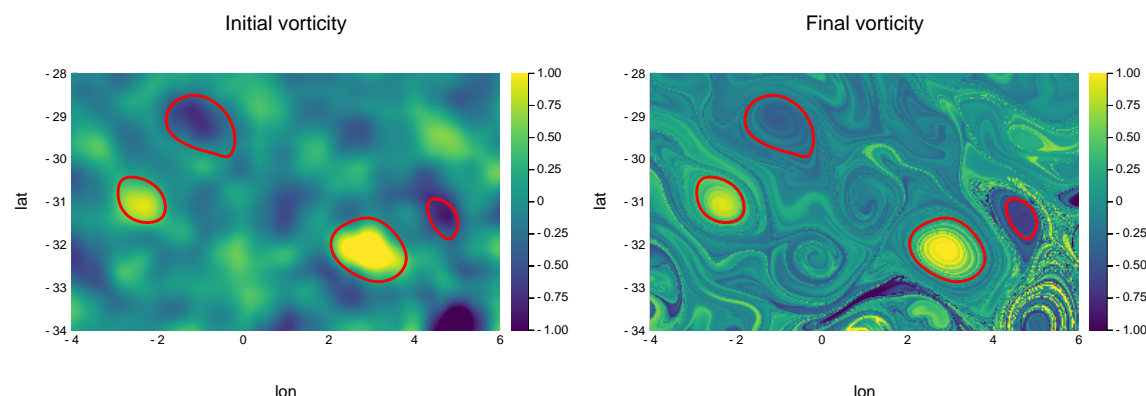
Figure 8.3. *Closed, constrained vorticity transport barriers in the AVISO ocean surface data set. The scalar field corresponds to vorticity (truncated at ± 1 for visualization purposes) at the initial (left) and the final (right) time instances in Lagrangian coordinates.*

9. Conclusions. We have shown how recent results on barriers to diffusive transport extend from the incompressible case treated in [15] to compressible flows. In our present setting, we have also allowed for the presence of sources and sinks in the concentration field. In addition, we have distinguished between the case of an unknown initial concentration (unconstrained extremizers) and the case of a specifically known initial concentration field (constrained extremizers) with respect to which diffusive transport is to be extremized over material surfaces.

For unconstrained barriers, we have obtained results that formally coincide with those in [15], except that the flow map here is compressible and the initial density of the fluid appears in the transport tensor. Despite the similarity with the results in [15], the present results have required a different derivation and additional assumptions on the selection of the most diffusion-prone initial concentration field near each material surface in the flow. In this formulation, concentration sinks and sources turn out to play no explicit role in the leading-order transport extremization problem. As in the incompressible case, we have obtained explicit direction fields defining the barriers for two-dimensional flows. For higher-dimensional flows, the barriers continue to be null-surfaces of a tensor field but satisfy PDEs. In any dimension, however, the DBS field can directly be computed from the velocity field and serves as a diagnostic to map out the global barrier distribution.

For constrained barriers, we have sought material surfaces that block transport more than their neighbors do under a specific initial concentration field. In this case, the equations defining the diffusion extremizers depend explicitly on the sink or source distribution for the concentration, as well as on the (possibly time-dependent) spontaneous concentration decay rate. Constrained barrier surfaces also satisfy explicit differential equations in two dimensions and PDEs in higher dimensions. A DBS scalar field is again available in any dimensions for diagnostic purposes. We have found in canonical examples that some classically documented transport barriers (such as jet cores and unstable manifolds) are, in fact, perfect enhancers of diffusive transport. Barriers that are strict local minimizers of diffusive transport, by contrast, are rare and must completely block transport at leading order, such as the walls of a channel

flow. In two dimensions, with the exception of perfect barriers, constrained uniform barriers are local maximizers of diffusive transport with respect to all localized perturbations.

Finally, we have shown how the above results extend to barriers to the transport of probability densities for particle motion in compressible, stochastic velocity fields modeled by Itô processes. This extension enables one to locate barriers to stochastic transport from purely deterministic calculations, as long as the diffusivities involved are small, which is generally the case for geophysical flows.

As we illustrated on two explicitly known Navier–Stokes flows, the present results on constrained barriers enable the detection of barriers to the diffusion of vorticity in two-dimensional flows. This follows because planar vorticity transport is governed by an (incompressible) advection-diffusion equation whose initial condition (the initial vorticity) cannot be considered unknown or uncertain once the velocity field is known. Barriers to vorticity diffusion in three dimensions, however, cannot be treated by the present results, given that vorticity is an active vector field, rather than a passively diffusing scalar field, in three-dimensional flows. More generally, the construction of barriers to the transport of active scalar and vector fields requires new ideas relative to those in the present work.

Appendix A. Proof of Theorem 1. We start by establishing an expression for the instantaneous flux vector associated with the transport of μ through a material surface. We consider first the transport of μ out of an arbitrary, closed material volume $V(t)$ to obtain an expression for the flux of μ through $\partial V(t)$ via the divergence theorem. The rate of change in the mass-based concentration of μ in a closed material volume $V(t) = \mathbf{F}_{t_0}^t \left(V(t) \right)$ is, by definition,

$$\frac{d}{dt} \int_{V(t)} \mu(\mathbf{x},t)\rho(\mathbf{x},t)dV = \frac{d}{dt} \int_{V(t_0)} \mu(\mathbf{F}_{t_0}^t(\mathbf{x}_0),t)\rho_0(\mathbf{x}_0)\, dV_0 = \int_{V(t_0)} \partial_t \hat{\mu}(\mathbf{x}_0,t)\rho_0(\mathbf{x}_0)\, dV_0$$

$$= \nu \int_{V(t_0)} \boldsymbol{\nabla}_0 \cdot \left[\mathbf{T}_{t_0}^t(\mathbf{x}_0)\boldsymbol{\nabla}_0 \left(\hat{\mu}(\mathbf{x}_0,t) + b(\mathbf{x}_0,t) \right) \right]\, dV_0$$

(A.1)
$$= \nu \int_{\partial V(t_0)} \left\langle \mathbf{T}_{t_0}^t \boldsymbol{\nabla}_0 \left(\hat{\mu}(\mathbf{x}_0,t) + b(\mathbf{x}_0,t) \right), \mathbf{n}_0 \right\rangle\, dA_0,$$

with the last integral denoting the surface integral over the $(n-1)$-dimensional boundary $\partial V(t_0)$ of the n-dimensional volume $V(t_0)$.

The flux formula (A.1) establishes that for an arbitrary volume $V(t_0)$, the flux vector of μ along the closed material surface $\partial V(t_0)$ is $\mathbf{T}_{t_0}^t \boldsymbol{\nabla}_0 \left(\hat{\mu}(\mathbf{x}_0,t) + b(\mathbf{x}_0,t) \right)$. For any open initial material surface $\mathcal{M}(t_0)$, we can select another open material surface $\mathcal{N}_0$ such that the closure of $\mathcal{M}(t_0) \cup \mathcal{N}_0$ is a closed material surface, i.e., $\partial V(t_0) = \overline{\mathcal{M}(t_0) \cup \mathcal{N}_0}$ is the boundary of a volume $V(t_0)$. Given that the flux of μ through $\partial V(t_0)$ is given by the final integral in (A.1) and hence is additive over subsets of $\partial V(t_0)$, the contribution of $\mathcal{M}(t_0)$ to the total flux through $\partial V(t_0)$ is equal to

(A.2)
$$\Sigma_{t_0}^{t_1}(\mathcal{M}_0) = \nu \int_{t_0}^{t_1} \int_{\mathcal{M}(t_0)} \left\langle \mathbf{T}_{t_0}^t \boldsymbol{\nabla}_0 \left(\hat{\mu}(\mathbf{x}_0,t) + b(\mathbf{x}_0,t) \right), \mathbf{n}_0 \right\rangle\, dA_0 dt,$$

with $\mathbf{n}_0(\mathbf{x}_0)$ denoting an oriented unit normal field to $\mathcal{M}(t_0)$.

To obtain more insight into $\Sigma_{t_0}^{t_1}(\mathcal{M}_0)$, we first take the $\boldsymbol{\nabla}_0$-gradient of both sides of (3.3) and integrate in time to obtain

$$(A.3) \quad \boldsymbol{\nabla}_0\hat{\mu}(\mathbf{x}_0, t) = \boldsymbol{\nabla}_0 c_0(\mathbf{x}_0) + \nu \int_{t_0}^{t} \boldsymbol{\nabla}_0 \left[\frac{1}{\rho_0(\mathbf{x}_0)} \boldsymbol{\nabla}_0 \cdot \left(\mathbf{T}_{t_0}^{s}(\mathbf{x}_0) \boldsymbol{\nabla}_0 \left[\hat{\mu}(\mathbf{x}_0, s) + b(\mathbf{x}_0, s) \right] \right) \right] ds,$$

where we have used the relation $\boldsymbol{\nabla}_0\hat{\mu}(\mathbf{x}_0, t_0) = \boldsymbol{\nabla}_0 c(\mathbf{x}_0)$, which follows from (3.1). Then with the flux vector obtained in (A.2) and with the expression (A.3) for $\boldsymbol{\nabla}_0\hat{\mu}(\mathbf{x}_0, t)$ at hand, the total transport of μ through $\mathcal{M}(t)$ can be written as

(A.4)

$$\Sigma_{t_0}^{t_1}(\mathcal{M}_0) = \nu \int_{t_0}^{t_1} \int_{\mathcal{M}_0} \left\langle \mathbf{T}_{t_0}^{t}(\mathbf{x}_0) \boldsymbol{\nabla}_0 \left(\hat{\mu}(\mathbf{x}_0, t) + b(\mathbf{x}_0, t) \right), \mathbf{n}_0(\mathbf{x}_0) \right\rangle \, dA_0 \, dt$$

$$= \nu \int_{t_0}^{t_1} \int_{\mathcal{M}_0} \left\langle \mathbf{T}_{t_0}^{t} \left(\boldsymbol{\nabla}_0 c_0(\mathbf{x}_0) + \boldsymbol{\nabla}_0 b(\mathbf{x}_0, t) \right), \mathbf{n}_0 \right\rangle \, dA_0 \, dt$$

$$+ \nu^2 \int_{t_0}^{t_1} \int_{\mathcal{M}_0} \int_{t_0}^{t} \boldsymbol{\nabla}_0 \left[\frac{1}{\rho_0(\mathbf{x}_0)} \boldsymbol{\nabla}_0 \cdot \left(\mathbf{T}_{t_0}^{s}(\mathbf{x}_0) \boldsymbol{\nabla}_0 \left[\hat{\mu}(\mathbf{x}_0, s) + b(\mathbf{x}_0, s) \right] \right) \right]^{T} \mathbf{T}_{t_0}^{s} \mathbf{n}_0 \, ds \, dA_0 \, dt.$$

The statement of the theorem, therefore, follows if the last term in (A.4) is of order $o(\nu)$, i.e., if

(A.5)

$$\lim_{\nu \to 0} \nu \int_{t_0}^{t_1} \int_{\mathcal{M}_0} \int_{t_0}^{t} \boldsymbol{\nabla}_0 \left[\frac{1}{\rho_0(\mathbf{x}_0)} \boldsymbol{\nabla}_0 \cdot \left(\mathbf{T}_{t_0}^{s}(\mathbf{x}_0) \boldsymbol{\nabla}_0 \left[\hat{\mu}(\mathbf{x}_0, s) + b(\mathbf{x}_0, s) \right] \right) \right]^{T} \mathbf{T}_{t_0}^{s} \mathbf{n}_0 \, ds \, dA_0 \, dt = 0.$$

To prove (A.5), we need estimates on the solution of the initial value problem

$$(A.6) \qquad \partial_t \hat{\mu}(\mathbf{x}_0, t) = \nu \frac{1}{\rho_0(\mathbf{x}_0)} \boldsymbol{\nabla}_0 \cdot \left(\mathbf{T}_{t_0}^{t}(\mathbf{x}_0) \boldsymbol{\nabla}_0 \left[\hat{\mu}(\mathbf{x}_0, t) + b(\mathbf{x}_0, t) \right] \right),$$

$$\hat{\mu}(\mathbf{x}_0, t_0) = c_0(\mathbf{x}_0).$$

Based on our initial assumptions, we have the following bounds on the entries $T_{ij}(\mathbf{x}_0, t) := \left[\mathbf{T}_{t_0}^{t}(\mathbf{x}_0) \right]_{ij}$ of the matrix representation of $\mathbf{T}_{t_0}^{t}$:

$$(A.7) \qquad \begin{aligned} \left| \rho_0(\mathbf{x}_0)^{-1} T_{ij}(\mathbf{x}_0, t) - \rho_0(\mathbf{y}_0)^{-1} T_{ij}(\mathbf{y}_0, s) \right| &\leq (C_1 \left| \mathbf{x}_0 - \mathbf{y}_0 \right|^{\alpha} + C_2 \left| t - s \right|^{\frac{\alpha}{2}}), \\ \left| \rho_0(\mathbf{x}_0)^{-1} \boldsymbol{\nabla}_0 T_{ij}(\mathbf{x}_0, t) - \rho_0(\mathbf{y}_0)^{-1} \boldsymbol{\nabla}_0 T_{ij}(\mathbf{y}_0, t) \right| &\leq C_3 | \mathbf{x}_0 - \mathbf{y}_0 |^{\alpha}, \end{aligned}$$

for some constant $0 < \alpha \leq 1$ and for all $\mathbf{x}_0, \mathbf{y}_0 \in U$ and $t, s \in [t_0, t_1]$. By the positive definiteness of $\mathbf{T}_{t_0}^{t}(\mathbf{x}_0)$ and the positivity of ρ_0, we also have

$$(A.8) \qquad \lambda |\mathbf{u}|^2 \leq \left\langle \mathbf{u}, \frac{1}{\rho_0(\mathbf{x}_0)} \mathbf{T}_{t_0}^{t}(\mathbf{x}_0) \mathbf{u} \right\rangle \leq \Lambda |\mathbf{u}|^2, \quad \mathbf{u} \in \mathbb{R}^n, \ \mathbf{x}_0 \in U, \ t \in [t_1, t_2],$$

which implies the bounds

$$(A.9) \qquad \frac{|\mathbf{u}|^2}{\Lambda} \leq \left\langle \mathbf{u}, \rho_0(\mathbf{x}_0) \left[\mathbf{T}_{t_0}^{t}(\mathbf{x}_0) \right]^{-1} \mathbf{u} \right\rangle \leq \frac{|\mathbf{u}|^2}{\lambda}, \quad \lambda^n \leq \rho_0(\mathbf{x}_0)^{-n} \det \mathbf{T}_{t_0}^{t}(\mathbf{x}_0) \leq \Lambda^n,$$

for all $\mathbf{u} \in \mathbb{R}^n$, $\mathbf{x}_0 \in U$, and $t \in [t_1, t_2]$.

Next, we observe that (A.5) is satisfied when

$$
(A.10) \qquad \sup_{\mathbf{x}_0 \in U, t \in [t_0, t_1]} |\boldsymbol{\nabla}_0 \hat{\mu}(\mathbf{x}_0, t) - \boldsymbol{\nabla}_0 c_0(\mathbf{x}_0)| = \mathcal{O}(\nu^q)
$$

holds for some $q > 0$, as one obtains using (A.3) and estimating the supremum norm in $\mathbf{x}_0$ and t using (A.7). Using the assumption that $c_0 \in C^2(U)$, we will now show that (A.10) holds, and hence (A.5) is indeed satisfied. In our presentation, we will utilize a scaling approach described by Friedman [9].

Introducing the rescaled time variable $\tau := \nu(t - t_0)$ as well as the shifted and rescaled concentration $w(\mathbf{x}_0, \tau) := \hat{\mu}(\mathbf{x}_0, t_0 + \frac{\tau}{\nu}) - c_0(\mathbf{x}_0)$, then setting $\mathbf{T}_\nu(\mathbf{x}_0, \tau) := \mathbf{T}_{t_0}^{t_0 + \frac{\tau}{\nu}}(\mathbf{x}_0)$, we can rewrite (A.6) as

$$
(A.11) \qquad \begin{cases} w_\tau = \frac{1}{\rho_0} \boldsymbol{\nabla}_0 \cdot (\mathbf{T}_\nu \boldsymbol{\nabla}_0 w) + \frac{1}{\rho_0} \boldsymbol{\nabla}_0 \cdot (\mathbf{T}_\nu \boldsymbol{\nabla}_0 (c_0 + b)), \\ w(\mathbf{x}_0, 0) = 0, \quad (\mathbf{x}_0, \tau) \in U \times [0, \nu(t_1 - t_0)]. \end{cases}
$$

Condition (A.10) is then equivalent to

$$
(A.12) \qquad \sup_{\mathbf{x}_0 \in \Omega, t \in [0, \tau_1]} |\boldsymbol{\nabla}_0 w(\mathbf{x}_0, \tau)| = \mathcal{O}(\nu^q), \qquad \tau_1 := \nu(t_1 - t_0),
$$

for some $q > 0$. In nondivergence form, (A.11) takes the form

$$
(A.13) \qquad w_\tau = \sum_{i,j=1}^{n} \frac{T_\nu^{ij}}{\rho_0} \frac{\partial^2 w}{\partial x_0^i \partial x_0^j} + \sum_{i=1}^{n} \frac{1}{\rho_0} \left(\sum_{j=1}^{n} \frac{\partial T_\nu^{ij}}{\partial x_0^j} \right) \frac{\partial w}{\partial x_0^i} + f_\nu,
$$

where we have defined

$$
(A.14) \qquad f_\nu(\mathbf{x}_0, \tau) := \frac{1}{\rho_0(\mathbf{x}_0)} \boldsymbol{\nabla}_0 \cdot (\mathbf{T}_\nu(\mathbf{x}_0, \tau) \boldsymbol{\nabla}_0 (c_0(\mathbf{x}_0) + b(\mathbf{x}_0, \tau))).
$$

Let

$$
(A.15) \qquad Z(\mathbf{x}_0, \tau; \boldsymbol{\xi}, s) := \frac{\exp\left[-\frac{\langle \mathbf{x}_0 - \boldsymbol{\xi}, \rho_0 \mathbf{T}_\nu^{-1}(\boldsymbol{\xi}, s)(\mathbf{x}_0 - \boldsymbol{\xi}) \rangle}{4(\tau - s)} \right]}{(2\sqrt{\pi})^n \left[\rho_0^{-n} \det \mathbf{T}_\nu(\boldsymbol{\xi}, s) \right]^{\frac{1}{2}} (\tau - s)^{\frac{n}{2}}},
$$

$$
Z_\tau = \rho_0^{-1} \mathbf{T}_\nu \boldsymbol{\nabla}_0^2 Z,
$$

for $\mathbf{x}_0, \boldsymbol{\xi} \in \Omega$ and $\tau, s \in [0, \tau_1]$, denote the fundamental solution of the homogeneous, second-order part of (A.11). For later computations, we note that with the n-dimensional volume element $d\boldsymbol{\xi} = d\xi_1 \dots d\xi_n$, we have the estimate

$$
\int_\Omega Z(\mathbf{x}_0, \tau; \boldsymbol{\xi}, s) \, d\boldsymbol{\xi} = \int_\Omega (2\sqrt{\pi})^{-n} \left[\rho_0^n \det \mathbf{T}_\nu^{-1} \right]^{-\frac{1}{2}} (\tau - s)^{-\frac{n}{2}} \mathrm{e}^{-\frac{\langle \mathbf{x}_0 - \boldsymbol{\xi}, \rho_0 \mathbf{T}_\nu^{-1}(\mathbf{x}_0 - \boldsymbol{\xi}) \rangle}{4(\tau - s)}} \, d\boldsymbol{\xi}
$$

$$
(A.16) \qquad \leq \int_\Omega (2\sqrt{\pi})^{-n} \lambda^{-\frac{n}{2}} (\tau - s)^{-\frac{n}{2}} \mathrm{e}^{-\frac{|\mathbf{x}_0 - \boldsymbol{\xi}|^2}{4\Lambda(\tau - s)}} \, d\boldsymbol{\xi},
$$

where we have used the inequalities in (A.9). With the rescaled spatial variable $\mathbf{y}$ and the rescaled volume form $d\mathbf{y}$ defined as

$$
(A.17) \qquad \mathbf{y} = (2\Lambda)^{-\frac{1}{2}}(\tau - s)^{-1/2}(\mathbf{x} - \boldsymbol{\xi}), \quad d\mathbf{y} = (2\Lambda)^{-\frac{n}{2}}(\tau - s)^{-\frac{n}{2}} d\boldsymbol{\xi},
$$

we define the set $\Omega_{\mathbf{x}_0,\tau,s} := (2\Lambda)^{-\frac{1}{2}}(\tau - s)^{-1/2}(\mathbf{x}_0 - \Omega)$ to obtain from (A.16) the estimate

$$
\begin{aligned}
\int_\Omega Z(\mathbf{x}_0, \tau; \boldsymbol{\xi}, s)\, d\boldsymbol{\xi} &\leq \pi^{-\frac{n}{2}} \left(\frac{\Lambda}{\lambda}\right)^{\frac{n}{2}} \int_{\Omega_{\mathbf{x},\tau,s}} \mathrm{e}^{-|\mathbf{y}|^2}\, d\mathbf{y} \\
&\leq \pi^{-\frac{n}{2}} \left(\frac{\Lambda}{\lambda}\right)^{\frac{n}{2}} \int_{\mathbb{R}^n} \mathrm{e}^{-|\mathbf{y}|^2}\, d\mathbf{y} = \left(\frac{\Lambda}{\lambda}\right)^{\frac{n}{2}},
\end{aligned}
\tag{A.18}
$$

where we have used that $\int_{-\infty}^{\infty} \mathrm{e}^{-r^2}\, dr = \sqrt{\pi}$. We also recall from [9, Thm. 3, p. 8], that for any continuous function $f : \bar{\Omega} \times [0, \tau_1] \to \mathbb{R}$, the integral

$$
(A.19) \qquad V(\mathbf{x}_0, \tau) := \int_0^\tau \int_\Omega Z(\mathbf{x}_0, \tau; \boldsymbol{\xi}, s) f(\boldsymbol{\xi}, s)\, d\boldsymbol{\xi} ds
$$

is continuously differentiable with respect to $\mathbf{x}_0$ and satisfies

$$
(A.20) \qquad \boldsymbol{\nabla}_0 V(\mathbf{x}_0, \tau) = \int_0^\tau \int_\Omega \boldsymbol{\nabla}_0 Z(\mathbf{x}_0, \tau; \boldsymbol{\xi}, s) f(\mathbf{x}_0, s)\, d\boldsymbol{\xi} ds.
$$

As shown in [9, Thm. 9, p. 21], the variation of constants formula applied to (A.11) gives its solution in the form

$$
\begin{aligned}
w(\mathbf{x}_0, \tau) &= \int_0^\tau \int_\Omega Z \boldsymbol{\nabla}_0 \cdot \left(\rho_0^{-1} \mathbf{T}_\nu \boldsymbol{\nabla}_0 c_0\right)\, d\boldsymbol{\xi}\, ds \\
&\quad + \int_0^\tau \int_\Omega Z(\mathbf{x}_0, \tau; \boldsymbol{\xi}, s) \\
&\quad \times \left(\int_0^s \int_\Omega \Phi(\boldsymbol{\xi}, s; \boldsymbol{\eta}, \sigma) \left(\rho_0^{-1} \mathbf{T}_\nu(\boldsymbol{\eta}, \sigma) \boldsymbol{\nabla}_0(c_0(\boldsymbol{\eta}) + b)\right)\, d\boldsymbol{\eta}\, d\sigma\right) d\boldsymbol{\xi}\, ds \\
&=: W_1(\mathbf{x}_0, \tau) + W_2(\mathbf{x}_0, \tau),
\end{aligned}
\tag{A.21}
$$

for some (not explicitly known) function Φ that satisfies the estimate

$$
(A.22) \qquad |\Phi(\boldsymbol{\xi}, s; \boldsymbol{\eta}, \sigma)| \leq C_4 \frac{1}{|s - \sigma|^{h_0}} \frac{1}{|\boldsymbol{\xi} - \boldsymbol{\eta}|^{n+2-2h_0-\alpha}},
$$

for any constant $h_0 \in \left(1 - \frac{\alpha}{2}, 1\right)$, where α is the Hölder exponent in (A.7).

To estimate the spatial gradient of W_1, we use the formula for the $\mathbf{x}_0$-derivative of (A.21) in (A.20) to obtain

$$
\begin{aligned}
|\boldsymbol{\nabla}_0 W_1| &= \left|\boldsymbol{\nabla}_0 \int_0^\tau \int_\Omega Z \boldsymbol{\nabla}_0 \cdot \left(\rho_0^{-1} \mathbf{T}_\nu \boldsymbol{\nabla}_0(c_0 + b)\right)\, d\boldsymbol{\xi}\, ds\right| \\
&= \left|\int_0^\tau \int_\Omega (\boldsymbol{\nabla}_0 Z) \boldsymbol{\nabla}_0 \cdot \left(\rho_0^{-1} \mathbf{T}_\nu \boldsymbol{\nabla}_0(c_0 + b)\right)\, d\boldsymbol{\xi}\, ds\right| \\
&\leq \int_0^\tau \int_\Omega \frac{1}{2|\tau - s|} \left|\rho_0 \mathbf{T}_\nu^{-1}(\boldsymbol{\xi}, s)(\mathbf{x}_0 - \boldsymbol{\xi})\right| |Z| \left|\boldsymbol{\nabla}_0 \cdot \left(\rho_0^{-1} \mathbf{T}_\nu \boldsymbol{\nabla}_0(c_0 + b)\right)\right|\, d\boldsymbol{\xi}\, ds,
\end{aligned}
\tag{A.23}
$$

where we also used the definition (A.15) in evaluating $\boldsymbol{\nabla}_0 Z$. From (A.9), we obtain $\|\rho_0 \mathbf{T}_\nu^{-1}\| = \lambda^{-1}$, and hence we can further write (A.23) as

$$
\begin{aligned}
|\boldsymbol{\nabla}_0 W_1| &\leq \frac{1}{\lambda} \int_0^\tau \int_\Omega \frac{|Z|}{2\,|\tau - s|} \left| \boldsymbol{\nabla}_0 \cdot \left(\rho_0^{-1} \mathbf{T}_\nu \boldsymbol{\nabla}_0 (c_0 + b) \right) \right| \, d\boldsymbol{\xi} \, ds \\
&\leq \frac{\| \boldsymbol{\nabla}_0 \cdot \left(\rho_0^{-1} \mathbf{T}_\nu \boldsymbol{\nabla}_0 (c_0 + b) \right) \|_{C^0(\Omega)}}{\lambda} \int_0^\tau \int_\Omega \frac{1}{2|\tau - s|} |\mathbf{x}_0 - \boldsymbol{\xi}| \, |Z| \, d\boldsymbol{\xi} \, ds \\
&\leq C_5 \frac{\|u_0\|_{C^2(\Omega)}}{\lambda} \int_0^\tau \int_\Omega \frac{1}{2|\tau - s|} |\mathbf{x}_0 - \boldsymbol{\xi}| \, |Z| \, d\boldsymbol{\xi} \, ds.
\end{aligned}
\tag{A.24}
$$

Next, as in the calculation of the integral in (A.16), we use the scaling (A.17) in (A.24) to obtain

$$
\begin{aligned}
|\boldsymbol{\nabla}_0 W_1| &\leq C_5 \frac{\Lambda \|u_0\|_{C^2(\Omega)}}{\lambda} \int_0^\tau \frac{1}{\sqrt{\tau - s}} \left(\int_{\mathbb{R}^n} |\boldsymbol{y}| \mathrm{e}^{-|\boldsymbol{y}|^2} \, d\boldsymbol{y} \right) ds \\
&\leq C_6 \frac{\Lambda \|u_0\|_{C^2(\Omega)}}{\lambda} \int_0^\tau \frac{1}{\sqrt{\tau - s}} \, ds \\
&\leq C_7 \sqrt{\tau} = \mathcal{O}\left(\nu^{\frac{1}{2}} \right).
\end{aligned}
\tag{A.25}
$$

To estimate the spatial gradient of W_2 in (A.21), we proceed similarly by using the growth condition (A.22) to obtain

$$
\begin{aligned}
|\boldsymbol{\nabla}_0 W_2| &\leq \int_0^\tau \int_\Omega \frac{1}{2\,|\tau - s|} \left| \rho_0 \mathbf{T}_\nu^{-1} (\mathbf{x}_0 - \boldsymbol{\xi}) \right| |Z| \\
&\qquad \times \left(\int_0^s \int_\Omega |\Phi| \left| \boldsymbol{\nabla}_0 \cdot \left(\rho_0^{-1} \mathbf{T}_\nu \boldsymbol{\nabla}_0 (c_0 + b) \right) \right| \, d\boldsymbol{\eta} \, d\sigma \right) d\boldsymbol{\xi} \, ds \\
&\leq C_8 \frac{\| \boldsymbol{\nabla}_0 \cdot \left(\rho_0^{-1} \mathbf{T}_\nu \boldsymbol{\nabla}_0 (c_0 + b) \right) \|_{C^0(\Omega)}}{\lambda} \\
&\qquad \times \int_0^\tau \int_\Omega \frac{1}{2|\tau - s|} |\mathbf{x}_0 - \boldsymbol{\xi}| \, |Z| \\
&\qquad \times \left(\int_0^s \frac{d\sigma}{|s - \sigma|^{h_0}} \int_\Omega \frac{d\boldsymbol{\eta}}{|\boldsymbol{\xi} - \boldsymbol{\eta}|^{n + 2 - 2h_0 - \alpha}} \right) d\boldsymbol{\xi} \, ds.
\end{aligned}
\tag{A.26}
$$

Since Ω is bounded, there exists a ball of radius R such that $\Omega + \Omega \subset B_R$ and therefore, noticing that $2 - 2h_0 - \alpha > 0$ by $1 - \frac{\alpha}{2} < h_0 < 1$, we find that

$$
\int_\Omega \frac{d\boldsymbol{\eta}}{|\boldsymbol{\xi} - \boldsymbol{\eta}|^{n + 2 - 2h_0 - \alpha}} \leq C_9 \left. r^{2 - 2h_0 - \alpha} \right|_{r=0}^{r=R} = C_9 R^{2 - 2h_0 - \alpha}.
\tag{A.27}
$$

As in (A.23), we can estimate the integral of $|\mathbf{x}_0 - \boldsymbol{\xi}|\,|Z|$ to obtain

$$
\begin{aligned}
|\boldsymbol{\nabla}_0 W_2| &\leq C_9 \frac{R^{2-2h_0-\alpha}\|u_0\|_{C^2(\Omega)}}{\lambda} \\
&\quad \times \int_0^\tau \int_\Omega \frac{1}{2|\tau - s|}\,|\mathbf{x}_0 - \boldsymbol{\xi}|\,|Z|\left(\int_0^s \frac{d\sigma}{|s-\sigma|^{h_0}}\right) d\boldsymbol{\xi}\, ds \\
&\leq C_{10} \frac{R^{2-2h_0-\alpha}\|u_0\|_{C^2(\Omega)}}{\lambda} \int_0^\tau \frac{1}{\sqrt{\tau - s}}\left(\int_0^s \frac{1}{|s-\sigma|^{h_0}}\,d\sigma\right) ds \\
&\leq C_{11} \int_0^\tau \frac{|\tau - s|^{1-h_0}}{\sqrt{\tau - s}}\,ds \\
&\leq C_{12}|\tau|^{\frac{3}{2}-h_0} = \mathcal{O}\left(\nu^{\frac{\alpha+1}{2}}\right).
\end{aligned}
$$

(A.28)

The estimates (A.25)–(A.28) together prove (A.12), which then implies (A.10), which in turn implies (A.5), as claimed.

Appendix B. Proof of Theorem 4. Applying the classic result on the variational derivative of quotient functional (see, e.g., [5]), we obtain that (5.3) is equivalent to

(B.1)

$$
\delta\tilde{\mathcal{E}}(\mathcal{M}_0) = \frac{1}{\int_{\mathcal{M}_0} dA_0}\delta \int_{\mathcal{M}_0} \left[\left|\left\langle \bar{\mathbf{q}}_{t_0}^{t_1}, \mathbf{n}_0\right\rangle\right| - \mathcal{T}_0\right] dA_0 = 0, \qquad \mathcal{T}_0 := \frac{\int_{\mathcal{M}_0} \left|\left\langle \bar{\mathbf{q}}_{t_0}^{t_1}, \mathbf{n}_0\right\rangle\right|\,dA_0}{\int_{\mathcal{M}_0} dA_0} = \text{const}
$$

Therefore, extrema of the functional

(B.2)

$$
\mathcal{E}(\mathcal{M}_0) := \int_{\mathcal{M}_0} \left[\left|\left\langle \bar{\mathbf{q}}_{t_0}^{t_1}, \mathbf{n}_0\right\rangle\right| - \mathcal{T}_0\right] dA_0
$$

coincide with those of $\tilde{\mathcal{E}}$.

We proceed by introducing a parametrization $\mathbf{x}_0(\mathbf{s}) := \mathbf{x}_0(s_1, \ldots s_{n-1})$ of $\mathcal{M}_0$ under which $\mathcal{E}(\mathcal{M}_0)$ becomes

(B.3)

$$
\mathcal{E}(\mathcal{M}_0) = \int_{\mathcal{M}_0} L\left(\mathbf{x}_0(\mathbf{s}), \partial_\mathbf{s}\mathbf{x}_0(\mathbf{s})\right) ds_1 \ldots ds_{n-1},
$$

with the Lagrangian

(B.4)

$$
L\left(\mathbf{x}_0, \partial_\mathbf{s}\mathbf{x}_0\right) := \left[\left|\left\langle \bar{\mathbf{q}}_{t_0}^{t_1}(\mathbf{x}_0), \mathbf{n}_0(\partial_\mathbf{s}\mathbf{x}_0)\right\rangle\right| - \mathcal{T}_0\right]\sqrt{\det \mathbf{G}(\partial_\mathbf{s}\mathbf{x}_0)}.
$$

Here $G_{ij} = \langle\frac{\partial\mathbf{x}_0}{\partial s_i}, \frac{\partial\mathbf{x}_0}{\partial s_j}\rangle$ denotes the (i,j) entry of the Gramian matrix $\mathbf{G}$ of the parametrization, which therefore satisfies, for any real number $c > 0$, the identity

$$
\sqrt{\det \mathbf{G}\left(\partial_{s_1}\mathbf{x}_0, \ldots, c\partial_{s_i}\mathbf{x}_0, \ldots, \partial_{s_{n-1}}\mathbf{x}_0\right)} = c\sqrt{\det \mathbf{G}(\partial_\mathbf{s}\mathbf{x}_0)}.
$$

Thus, by definition, $\sqrt{\det \mathbf{G}}$ is a positively homogeneous function of $\partial_{s_i}\mathbf{x}_0$ with order 1 and hence, by Euler's theorem [21], satisfies

(B.5)

$$
\partial_{s_i}\mathbf{x}_0(\mathbf{s}) \cdot \frac{\partial\sqrt{\det \mathbf{G}}}{\partial\left(\partial_{s_i}\mathbf{x}_0(\mathbf{s})\right)} = 1 \cdot \sqrt{\det \mathbf{G}} = \sqrt{\det \mathbf{G}}.
$$

Furthermore, once an orientation is fixed, the unit normal $\mathbf{n}_0$ is a unique smooth function of the $n-1$ tangent vectors $\partial_{s_i}\mathbf{x}_0$, even though the lengths of these vectors are arbitrary and depend on the parametrization. Consequently, for any real number $c > 0$, we have

$$\mathbf{n}_0\left(\partial_{s_1}\mathbf{x}_0,\ldots,c\partial_{s_i}\mathbf{x}_0,\ldots,\partial_{s_{n-1}}\mathbf{x}_0\right) = \mathbf{n}_0\left(\partial_{\mathbf{s}}\mathbf{x}_0\right) = c^k \cdot \mathbf{n}_0\left(\partial_{\mathbf{s}}\mathbf{x}_0(\mathbf{s})\right), \quad k = 0,$$

which, by definition, implies that $\mathbf{n}_0\left(\partial_{\mathbf{s}}\mathbf{x}_0(\mathbf{s})\right)$ is a positively homogeneous function of order zero. Then, again by Euler's theorem, we conclude that

$$(\text{B.6}) \qquad \partial_{s_i}\mathbf{x}_0(\mathbf{s}) \cdot \frac{\partial \mathbf{n}_0\left(\partial_{\mathbf{s}}\mathbf{x}_0(\mathbf{s})\right)}{\partial\left(\partial_{s_i}\mathbf{x}_0(\mathbf{s})\right)} = 0.$$

As the Lagrangian $L\left(\mathbf{x}_0,\partial_{\mathbf{s}}\mathbf{x}_0\right)$ has no explicit dependence on $\mathbf{s}$, Noether's theorem provides partial conservation laws (cf. Logan [22, Chap. 4, Ex. 4.2]) for the associated Euler–Lagrange equation in the form

$$(\text{B.7}) \qquad \frac{\partial H_j^i}{\partial s_k} = 0, \quad H_j^i := \partial_{s_j}\mathbf{x}_0 \cdot \frac{\partial L}{\partial\left(\partial_{s_i}\mathbf{x}_0\right)} - \delta_{ij}L, \quad i,j,k = 1,\ldots,n-1,$$

with δ_{ij} referring to the Kronecker delta. A direct calculation using (B.5)–(B.6), however, gives

$$\begin{aligned}
H_i^i &= \partial_{s_i}\mathbf{x}_0(\mathbf{s}) \cdot \frac{\partial L}{\partial\left(\partial_{s_i}\mathbf{x}_0(\mathbf{s})\right)} - L \\
&= \left[\left|\langle\bar{\mathbf{q}}_{t_0}^{t_1},\mathbf{n}_0\rangle\right| - \mathcal{T}_0\right]\partial_{s_i}\mathbf{x}_0(\mathbf{s}) \cdot \frac{\partial\sqrt{\det\mathbf{G}}}{\partial\left(\partial_{s_i}\mathbf{x}_0(\mathbf{s})\right)} - L \\
&= \left[\left|\langle\bar{\mathbf{q}}_{t_0}^{t_1}\left(\mathbf{x}_0\right),\mathbf{n}_0\left(\partial_{\mathbf{s}}\mathbf{x}_0\right)\rangle\right| - \mathcal{T}_0\right]\sqrt{\det\mathbf{G}\left(\partial_{\mathbf{s}}\mathbf{x}_0\right)} \\
&= 0,
\end{aligned}$$

and hence no nontrivial first integral arises from the relations (B.7).

Nevertheless, for the modified variational problem

$$(\text{B.8}) \qquad \hat{\mathcal{E}}(\mathcal{M}_0) = \int_{\mathcal{M}_0} L^2\left(\mathbf{x}_0(\mathbf{s}),\partial_{\mathbf{s}}\mathbf{x}_0(\mathbf{s})\right)\, ds_1 \ldots ds_{n-1},$$

Noether's theorem gives

$$(\text{B.9}) \qquad H_i^i := \partial_{s_i}\mathbf{x}_0 \cdot \frac{\partial L^2}{\partial\left(\partial_{s_i}\mathbf{x}_0\right)} - L^2 = 2L^2 - L^2 = L^2, \quad i = 1,\ldots,n-1,$$

by Euler's theorem, given that L^2 is a positively homogeneous function of order 2 in the variables $\partial_{s_i}\mathbf{x}_0$. By the definition of H_i^i in (B.7), (B.9) implies that L is a first integral for solutions of the variational problem (B.8). Then, by a generalization of the Maupertuis principle for PDEs (see [15, App. S4]), L is also a first integral for the Euler–Lagrange equation of the original variational problem on all nonzero level sets of L. This in turn implies the invariance of the $\{L = 0\}$ level set as well. We conclude that barrier surfaces must satisfy $\left[\left|\langle\bar{\mathbf{q}}_{t_0}^{t_1}\left(\mathbf{x}_0\right),\mathbf{n}_0\left(\partial_{\mathbf{s}}\mathbf{x}_0\right)\rangle\right| - \mathcal{T}_0\right]\sqrt{\det\mathbf{G}\left(\partial_{\mathbf{s}}\mathbf{x}_0\right)} = C$ in any dimension.

Appendix C. Proof of Theorem 5. For $n = 2$, a diffusion extremizer surface $\mathcal{M}_0$ is a one-dimensional curve parametrized by the single variable s. The unit normal to this curve at a point $\mathbf{x}_0 \in \mathcal{M}_0$ can be written as

$$\mathbf{n}_0(\mathbf{x}_0) = \mathbf{\Omega} \frac{\mathbf{x}_0'}{|\mathbf{x}_0'|},$$

with the rotation matrix $\mathbf{\Omega}$ defined as in (5.15). The Lagrangian L defined in (B.4) then takes the specific form

$$L\left(\mathbf{x}_0, \mathbf{x}_0'\right) = \left(\sqrt{\left\langle \bar{\mathbf{q}}_{t_0}^{t_1}\left(\mathbf{x}_0\right), \mathbf{\Omega} \frac{\mathbf{x}_0'}{|\mathbf{x}_0'|} \right\rangle^2} - \mathcal{T}_0 \right) \sqrt{\langle \mathbf{x}_0', \mathbf{x}_0' \rangle}$$

$$\text{(C.1)} \qquad = \sqrt{\left\langle \bar{\mathbf{q}}_{t_0}^{t_1}\left(\mathbf{x}_0\right), \mathbf{\Omega}\mathbf{x}_0' \right\rangle^2} - \mathcal{T}_0 \left| \mathbf{x}_0' \right|.$$

The general equation (5.4), therefore, simplifies in two dimensions to the implicit ODE

$$\text{(C.2)} \qquad \left| \left\langle \mathbf{\Omega}\bar{\mathbf{q}}_{t_0}^{t_1}\left(\mathbf{x}_0\right), \frac{\mathbf{x}_0'}{|\mathbf{x}_0'|} \right\rangle \right| = \mathcal{T}_0.$$

Note from (C.2) that within the $\{L = 0\}$ level set, arbitrary reparametrizations of the solutions (which are also solutions, by the rescaling invariance of the variational principle) also happen to preserve the value of the first integral L. We are, therefore, free to select the arc-length parametrization for diffusion barriers by letting $\mathbf{x}_0' = \alpha \bar{\mathbf{q}}_{t_0}^{t_1}\left(\mathbf{x}_0\right) + \beta \mathbf{\Omega}\bar{\mathbf{q}}_{t_0}^{t_1}\left(\mathbf{x}_0\right)$ with $\left(\alpha^2 + \beta^2\right) = 1/\left|\bar{\mathbf{q}}_{t_0}^{t_1}\left(\mathbf{x}_0\right)\right|^2$. Substituting this form of $\mathbf{x}_0'$ into (C.2) gives the vector field family

$$\text{(C.3)} \qquad \mathbf{x}_0' = \frac{\sqrt{\left|\bar{\mathbf{q}}_{t_0}^{t_1}\left(\mathbf{x}_0\right)\right|^2 - \mathcal{T}_0^2}}{\left|\bar{\mathbf{q}}_{t_0}^{t_1}\left(\mathbf{x}_0\right)\right|^2} \bar{\mathbf{q}}_{t_0}^{t_1}\left(\mathbf{x}_0\right) \pm \frac{\mathcal{T}_0}{\left|\bar{\mathbf{q}}_{t_0}^{t_1}\left(\mathbf{x}_0\right)\right|^2} \mathbf{\Omega}\bar{\mathbf{q}}_{t_0}^{t_1}\left(\mathbf{x}_0\right),$$

as stated in (5.17), where we have used the equality $\left|\mathbf{\Omega}\bar{\mathbf{q}}_{t_0}^{t_1}\right| = \left|\bar{\mathbf{q}}_{t_0}^{t_1}\right|$. Trajectories of (5.17) are, therefore, stationary curves of $\mathcal{E}$.

It is yet unclear, however, whether trajectories of (5.17) are minimizers or maximizers of the functional $\tilde{\mathcal{E}}$. As we have seen, stationary curves of $\tilde{\mathcal{E}}$ coincide with those of

$$\mathcal{E}(\mathcal{M}_0) = \int_{\mathcal{M}_0} L\left(\mathbf{x}_0(s), \mathbf{x}_0'(s)\right) ds,$$

with L defined in (C.1). As in any classic calculus of variations problem, the admissible variations $\mathbf{h}(s)$ of a $\mathcal{M}_0$ are those that make the boundary term arising in the integration by parts vanish, i.e.,

$$\text{(C.4)} \qquad \left[\partial_{\mathbf{x}_0'} L\left(\mathbf{x}_0(s), \mathbf{x}_0'(s)\right) \cdot \mathbf{h}(s) \right]_{s_1}^{s_2} = 0.$$

Noting that
(C.5)

$$\partial_{\mathbf{x}_0'} L\left(\mathbf{x}_0, \mathbf{x}_0'\right) = \text{sign} \left\langle \left\langle \bar{\mathbf{q}}_{t_0}^{t_1}\left(\mathbf{x}_0\right), \mathbf{\Omega}\mathbf{x}_0' \right\rangle \right\rangle \mathbf{\Omega}^T \bar{\mathbf{q}}_{t_0}^{t_1}\left(\mathbf{x}_0\right) - \mathcal{T}_0 \frac{\mathbf{x}_0'}{\sqrt{\langle \mathbf{x}_0', \mathbf{x}_0' \rangle}}, \quad \left\langle \bar{\mathbf{q}}_{t_0}^{t_1}\left(\mathbf{x}_0\right), \mathbf{\Omega}\mathbf{x}_0' \right\rangle \neq 0,$$

we can distinguish the following types of variations based on (C.4):

B1. *Vanishing endpoint variations*: $\mathbf{h}(s_1) = \mathbf{h}(s_2) = \mathbf{0}$.

B2. *Orthogonal endpoint variations*: The variation $\mathbf{h}(s)$ is nonzero but orthogonal to $\partial_{\mathbf{x}_0'} L\left(\mathbf{x}_0(s), \mathbf{x}_0'(s)\right)$ at the endpoints, i.e.,

$$(C.6) \qquad \partial_{\mathbf{x}_0'} L\left(\mathbf{x}_0(s_i), \mathbf{x}_0'(s_i)\right) \perp \mathbf{h}(s_i), \quad i = 1, 2.$$

Restricting to normal variations $(\mathbf{h}(s) \perp \mathbf{x}_0'(s))$ and using (C.5), we find that (C.6) is equivalent to

$$\boldsymbol{\Omega} \bar{\mathbf{q}}_{t_0}^{t_1}\left(\mathbf{x}_0(s_i)\right) \cdot \mathbf{h}(s_i) = 0, \quad i = 1, 2,$$

as long as $\left\langle \bar{\mathbf{q}}_{t_0}^{t_1}\left(\mathbf{x}_0\right), \boldsymbol{\Omega} \mathbf{x}_0' \right\rangle \neq 0$, i.e., as long as L is differentiable. We conclude that arbitrary normal variations are admissible to the endpoints of $\mathcal{M}_0$ whenever $\bar{\mathbf{q}}_{t_0}^{t_1}\left(\mathbf{x}_0(s_i)\right) \parallel \mathbf{x}_0'(s_i)$, $i = 1, 2$, holds at those endpoints.

B3. *Free endpoint variations*: The factor $\partial_{\mathbf{x}_0'} L\left(\mathbf{x}_0, \mathbf{x}_0'\right)$ vanishes at the endpoints, i.e.,

$$(C.7) \qquad \partial_{\mathbf{x}_0'} L\left(\mathbf{x}_0(s_i), \mathbf{x}_0'(s_i)\right) = \mathbf{0}, \quad i = 1, 2.$$

Using (C.5) and the expression (C.3) for $\mathbf{x}_0'$ along $\mathcal{M}_0$, we find that condition (C.7) is satisfied whenever

$$\partial_{\mathbf{x}_0'} L|_{\mathcal{M}_0} = -\left[\operatorname{sign} \left\langle \left\langle \bar{\mathbf{q}}_{t_0}^{t_1}\left(\mathbf{x}_0\right), \boldsymbol{\Omega} \mathbf{x}_0' \right\rangle \right\rangle \pm \mathcal{T}_0 \right] \boldsymbol{\Omega} \bar{\mathbf{q}}_{t_0}^{t_1}\left(\mathbf{x}_0\right) - \mathcal{T}_0 \frac{\sqrt{\left|\bar{\mathbf{q}}_{t_0}^{t_1}\left(\mathbf{x}_0\right)\right|^2 - \mathcal{T}_0^2}}{\left|\bar{\mathbf{q}}_{t_0}^{t_1}\left(\mathbf{x}_0\right)\right|^2} \bar{\mathbf{q}}_{t_0}^{t_1}\left(\mathbf{x}_0\right).$$

Therefore, condition (C.7) is satisfied if either

$$\bar{\mathbf{q}}_{t_0}^{t_1}\left(\mathbf{x}_0(s_i)\right) = \mathbf{0}, \quad i = 1, 2,$$

or

$$\mathcal{T}_0 = \left|\bar{\mathbf{q}}_{t_0}^{t_1}\left(\mathbf{x}_0(s_i)\right)\right| = 1, \quad i = 1, 2.$$

B4. *Periodic variations*: $\mathcal{M}_0$ is a closed curve and the variation $\mathbf{h}(s)$ is periodic with the same period in s, i.e.,

$$\partial_{\mathbf{x}_0'} L\left(\mathbf{x}_0(s_1), \mathbf{x}_0'(s_1)\right) \cdot \mathbf{h}(s_1) = \partial_{\mathbf{x}_0'} L\left(\mathbf{x}_0(s_2), \mathbf{x}_0'(s_2)\right) \cdot \mathbf{h}(s_2).$$

A simple calculation gives, furthermore, that the second variation of $\tilde{\mathcal{E}}$ along any of its stationary curves, $\mathcal{M}_0$, satisfies

$$\delta^2 \tilde{\mathcal{E}}(\mathcal{M}_0) = \frac{\delta^2 \mathcal{E}(\mathcal{M}_0)}{\int_{\mathcal{M}_0} \sqrt{\langle \mathbf{x}_0'(s), \mathbf{x}_0'(s) \rangle}\, ds}.$$

Therefore, $\tilde{\mathcal{E}}$ and $\mathcal{E}$ also share the type of their stationary curves (minimizers, maximizers, or saddle-type stationary curves). To obtain a necessary condition for a stationary curve of $\tilde{\mathcal{E}}$ to be an extremizer, we can therefore apply the classic Legendre condition to the functional $\mathcal{E}$, which is based on the definiteness of the Hessian $\partial^2_{\mathbf{x}_0' \mathbf{x}_0'} L\left(\mathbf{x}_0, \mathbf{x}_0'\right)$.

Note that whenever $\partial_{\mathbf{x}_0'} L\left(\mathbf{x}_0, \mathbf{x}_0'\right)$ is well-defined in (C.5), i.e., $\left\langle \bar{\mathbf{q}}_{t_0}^{t_1}\left(\mathbf{x}_0\right), \mathbf{\Omega}\mathbf{x}_0' \right\rangle \neq 0$ holds, the function sign $\left\langle \left\langle \bar{\mathbf{q}}_{t_0}^{t_1}\left(\mathbf{x}_0\right), \mathbf{\Omega}\mathbf{x}_0' \right\rangle \right\rangle$ is locally constant in $\mathbf{x}_0'$. Therefore, whenever $\partial_{\mathbf{x}_0'} L\left(\mathbf{x}_0, \mathbf{x}_0'\right)$ is differentiable, its Jacobian equals

$$
\begin{aligned}
(C.8) \qquad \partial_{\mathbf{x}_0' \mathbf{x}_0'}^2 L\left(\mathbf{x}_0, \mathbf{x}_0'\right) &= -\mathcal{T}_0 \partial_{\mathbf{x}_0'} \frac{\mathbf{x}_0'}{\sqrt{\langle \mathbf{x}_0', \mathbf{x}_0' \rangle}} \\
&= -\frac{\mathcal{T}_0}{\sqrt{\langle \mathbf{x}_0', \mathbf{x}_0' \rangle}} \left[\mathbf{I} - \frac{1}{\langle \mathbf{x}_0', \mathbf{x}_0' \rangle} \mathbf{x}_0' \left(\mathbf{x}_0'\right)^T \right], \quad \left\langle \bar{\mathbf{q}}_{t_0}^{t_1}\left(\mathbf{x}_0\right), \mathbf{\Omega}\mathbf{x}_0' \right\rangle \neq 0.
\end{aligned}
$$

Recall that any two-dimensional dyadic product matrix $\mathbf{x}_0' \left(\mathbf{x}_0'\right)^T$ has an eigenvalue equal to $\langle \mathbf{x}_0', \mathbf{x}_0' \rangle$ (corresponding to the eigenvector $\mathbf{x}_0'$) and another eigenvalue equal to zero (corresponding to $\mathbf{\Omega}\mathbf{x}_0'$). As a consequence, the eigenvalues of $\partial_{\mathbf{x}_0' \mathbf{x}_0'}^2 L\left(\mathbf{x}_0, \mathbf{x}_0'\right)$ are

$$
\rho_1 = 0, \quad \rho_2 = -\frac{\mathcal{T}_0}{\sqrt{\langle \mathbf{x}_0', \mathbf{x}_0' \rangle}} < 0,
$$

which implies that the Hessian $\partial_{\mathbf{x}_0' \mathbf{x}_0'}^2 L\left(\mathbf{x}_0, \mathbf{x}_0'\right)$ is negative semidefinite on any stationary curve of $\tilde{\mathcal{E}}$ satisfying $\left\langle \bar{\mathbf{q}}_{t_0}^{t_1}\left(\mathbf{x}_0\right), \mathbf{\Omega}\mathbf{x}_0' \right\rangle \neq 0$. (The kernel of $\partial_{\mathbf{x}_0' \mathbf{x}_0'}^2 L\left(\mathbf{x}_0, \mathbf{x}_0'\right)$ is spanned by $\mathbf{x}_0'$, confirming that tangential perturbations to the stationary curve at its endpoints result in no second-order change in the transport functional due to our length-normalized definition of transport.) Consequently, each stationary curve of $\tilde{\mathcal{E}}$ satisfies the Legendre necessary condition for a strict maximum.

For stationary curves $\mathcal{M}_0$ that either are closed or connect zeros of the $\bar{\mathbf{q}}_{t_0}^{t_1}\left(\mathbf{x}_0\right)$ vector field (cf. the boundary condition types B3 and B4 above), we now derive another necessary condition under which a closed stationary curve $\mathcal{M}_0$ is a local maximum of $\mathcal{E}$. We consider parallel translations of $\mathcal{M}_0$ described by a constant vector field $\mathbf{h}(s) \equiv \mathbf{h}_0$. Since we have $\mathbf{h}'(s) \equiv \mathbf{0}$ along such perturbations, we obtain

$$
\delta^2 \mathcal{E}[\mathbf{h}_0] = \frac{1}{2} \int_{\mathcal{M}_0} \left\langle \mathbf{h}_0, \partial_{\mathbf{x}_0 \mathbf{x}_0}^2 L(\mathbf{x}_0, \mathbf{x}_0')\mathbf{h}_0 \right\rangle ds = \frac{1}{2} \left\langle \mathbf{h}_0, \mathbf{L}\mathbf{h}_0 \right\rangle, \quad \mathbf{L} := \int_{\mathcal{M}_0} \partial_{\mathbf{x}_0 \mathbf{x}_0}^2 L\left(\mathbf{x}_0(s), \mathbf{x}_0'(s)\right) ds.
$$

Therefore, $\delta^2 \mathcal{E}[\mathbf{h}_0] \leq 0$ holds for arbitrary $\mathbf{h}_0$ if $\mathbf{L}$ is negative semidefinite. Note that wherever L is differentiable, its Hessian with respect to $\mathbf{x}_0$ satisfies

$$
\partial_{\mathbf{x}_0 \mathbf{x}_0}^2 L\left(\mathbf{x}_0, \mathbf{x}_0'\right) = \text{sign} \left\langle \bar{\mathbf{q}}_{t_0}^{t_1}\left(\mathbf{x}_0\right), \mathbf{\Omega}\mathbf{x}_0' \right\rangle \partial_{\mathbf{x}_0 \mathbf{x}_0}^2 \left\langle \bar{\mathbf{q}}_{t_0}^{t_1}\left(\mathbf{x}_0\right), \mathbf{\Omega}\mathbf{x}_0' \right\rangle,
$$

which then implies formula (5.18) of the theorem. The same argument is also valid for barriers with endpoints satisfying

$$
\bar{\mathbf{q}}_{t_0}^{t_1}\left(\mathbf{x}_0(s_i)\right) \parallel \mathbf{x}_0'(s_i) \parallel \mathbf{x}_0'(s_j), \quad i, j = 1, 2, \quad i \neq j
$$

(cf. the boundary conditions B2), except that in that case

$$
\left\langle \mathbf{L}\mathbf{\Omega}\mathbf{x}_0', \mathbf{\Omega}\mathbf{x}_0' \right\rangle \leq 0
$$

must hold for the stationary curve to be a minimizer, given that the admissible parallel translations are restricted to those normal translations satisfying $\mathbf{h}(s) \equiv \mathbf{h}_0 \perp \mathbf{x}_0'(s_i)$, $i = 1, 2$.

In summary, no trajectory of (5.17) can be a minimizer of the constrained transport functional $\mathcal{E}$ for $\mathcal{T}_0$. For $\mathcal{T}_0 = 0$, however, one recovers the case of perfect barriers that are clearly global minimizers of $\mathcal{E}$. Thus, only perfect barriers can be transport-minimizing material surfaces, as stated in Theorem 5.

REFERENCES

[1] S. BALASURIYA, N. T. OUELLETTE, AND I. I. RYPINA, *Generalized Lagrangian coherent structures*, Phys. D, 372 (2018), pp. 31–51, https://doi.org/10.1016/j.physd.2018.01.011.

[2] F. J. BERON-VERA, M. G. BROWN, M. J. OLASCOAGA, I. I. RYPINA, H. KOÇAK, AND I. A. UDOVY-DCHENKOV, *Zonal jets as transport barriers in planetary atmospheres*, J. Atmos. Sci., 65 (2008), pp. 3316–3326, https://doi.org/10.1175/2008JAS2579.1.

[3] J. BEZANSON, A. EDELMAN, S. KARPINSKI, AND V. B. SHAH, *Julia: A fresh approach to numerical computing*, SIAM Rev., 59 (2017), pp. 65–98, https://doi.org/10.1137/141000671.

[4] K. P. BOWMAN, *Large-scale isentropic mixing properties of the Antarctic polar vortex from analyzed winds*, J. Geophys. Res. Atmos., 98 (1993), pp. 23013–23027, https://doi.org/10.1029/93JD02599.

[5] E. CASTILLO, A. LUCEÑO, AND P. PEDREGAL, *Composition functionals in calculus of variations: Application to products and quotients*, Math. Models Methods Appl. Sci., 18 (2008), pp. 47–75, https://doi.org/10.1142/S0218202508002607.

[6] P. CHEN, *The permeability of the antarctic vortex edge*, J. Geophys. Res. Atmos., 99 (1994), pp. 20563–20571, https://doi.org/10.1029/94JD01754.

[7] E. A. D'ASARO, A. Y. SHCHERBINA, J. M. KLYMAK, J. MOLEMAKER, G. NOVELLI, C. M. GUIGAND, A. C. HAZA, B. K. HAUS, E. H. RYAN, G. A. JACOBS, H. S. HUNTLEY, N. J. M. LAXAGUE, S. CHEN, F. JUDT, J. C. MCWILLIAMS, R. BARKAN, A. D. KIRWAN, A. C. POJE, AND T. M. ÖZGÖKMEN, *Ocean convergence and the dispersion of flotsam*, Proc. Nat. Acad. Sci. USA, 115 (2018), pp. 1162–1167, https://doi.org/10.1073/pnas.1718453115.

[8] A. DINKLAGE, T. KLINGER, G. MARX, AND L. SCHWEIKHARD, *Plasma Physics—Confinement, Transport and Collective Effects*, Lecture Notes in Phys. 670, Springer, Berlin, 2005, https://doi.org/10.1007/b103882.

[9] A. FRIEDMAN, *Partial Differential Equations of Parabolic Type*, Dover, New York, 2013.

[10] G. FROYLAND AND E. KWOK, *A dynamic Laplacian for identifying Lagrangian coherent structures on weighted Riemannian manifolds*, J. Nonlinear Sci., (2017), https://doi.org/10.1007/s00332-017-9397-y.

[11] A. HADJIGHASEM, M. FARAZMAND, D. BLAZEVSKI, G. FROYLAND, AND G. HALLER, *A critical comparison of Lagrangian methods for coherent structure detection*, Chaos, 27 (2017), 053104, https://doi.org/10.1063/1.4982720.

[12] A. HADJIGHASEM AND G. HALLER, *Geodesic transport barriers in Jupiter's atmosphere: A video-based analysis*, SIAM Rev., 58 (2016), pp. 69–89, https://doi.org/10.1137/140983665.

[13] A. HADJIGHASEM AND G. HALLER, *Level set formulation of two-dimensional lagrangian vortex detection methods*, Chaos, 26 (2016), 103102, https://doi.org/10.1063/1.4964103.

[14] G. HALLER AND F. J. BERON-VERA, *Coherent Lagrangian vortices: The black holes of turbulence*, J. Fluid Mech., 731 (2013), R4, https://doi.org/10.1017/jfm.2013.391.

[15] G. HALLER, D. KARRASCH, AND F. KOGELBAUER, *Material barriers to diffusive and stochastic transport*, Proc. Nat. Acad. Sci. USA, 115 (2018), pp. 9074–9079, https://doi.org/10.1073/pnas.1720177115.

[16] D. KARRASCH, F. HUHN, AND G. HALLER, *Automated detection of coherent Lagrangian vortices in two-dimensional unsteady flows*, Proc. R. Soc. A, 471 (2015), 20140639, https://doi.org/10.1098/rspa.2014.0639.

[17] D. KARRASCH AND J. KELLER, *A Geometric Heat-Flow Theory of Lagrangian Coherent Structures*, preprint, https://arxiv.org/abs/1608.05598, 2016.

[18] D. KARRASCH AND N. SCHILLING, *Fast and Robust Computation of Coherent Lagrangian Vortices on Very Large Two-Dimensional Domains*, preprint, https://arxiv.org/abs/1907.08449, 2019.

[19] L. D. LANDAU AND E. LIFSHITZ, *Fluid Mechanics*, Pergamon Press, London, 1966.

[20] F. LEKIEN AND S. D. ROSS, *The computation of finite-time Lyapunov exponents on unstructured meshes and for non-Euclidean manifolds*, Chaos, 20 (2010), 017505, https://doi.org/10.1063/1.3278516.

[21] J. P. LEWIS, An Introduction to Mathematics for Students of Economics, Macmillan, London, 1969, *Homogeneous functions and Euler's theorem*, in pp. 297–303.

[22] J. D. LOGAN, *Invariant Variational Principles*, Math. Sci. Eng. 138, Academic Press, New York, 1977.

[23] R. S. MacKAY, *Transport in 3D volume-preserving flows*, J. Nonlinear Sci., 4 (1994), pp. 329–354, https://doi.org/10.1007/BF02430637.

[24] A. J. MAJDA AND A. L. BERTOZZI, *Vorticity and Incompressible Flow*, Cambridge Texts Appl. Math. 27, Cambridge University Press, Cambridge, UK, 2002.

[25] N. NAKAMURA, *Quantifying Inhomogeneous, Instantaneous, Irreversible Transport Using Passive Tracer Field as a Coordinate*, in Transport and Mixing in Geophysical Flows, Lecture Notes in Phys. 744, Springer, Berlin, 2008, pp. 137–164, https://doi.org/10.1007/978-3-540-75215-8_7.

[26] J. M. OTTINO, *The Kinematics of Mixing: Stretching, Chaos, and Transport*, Cambridge University Press, Cambridge, UK, 1989.

[27] L. PRATT, R. BARKAN, AND I. RYPINA, *Scalar flux kinematics*, Fluids, 1 (2016), https://doi.org/10.3390/fluids1030027.

[28] C. RACKAUCKAS AND Q. NIE, *DifferentialEquations.jl—A Performant and Feature-Rich Ecosystem for Solving Differential Equations in Julia*, J. Open Research Software, 5 (2017), https://doi.org/10.5334/jors.151.

[29] H. RISKEN, *The Fokker-Planck Equation: Methods of Solution and Applications*, Springer Ser. Synergetics 18, Springer, New York, 1984, https://doi.org/10.1007/978-3-642-61544-3.

[30] D. ROSNER, *Transport Processes in Chemically Reacting Flow Systems*, Dover, New York, 2000.

[31] M. SERRA AND G. HALLER, *Efficient computation of null geodesics with applications to coherent vortex detection*, Proc. R. Soc. A, 473 (2017), https://doi.org/10.1098/rspa.2016.0807.

[32] M. SERRA, P. SATHE, F. BERON-VERA, AND G. HALLER, *Uncovering the edge of the polar vortex*, J. Atmos. Sci., 74 (2017), pp. 3871–3885, https://doi.org/10.1175/JAS-D-17-0052.1.

[33] X. TANG AND A. BOOZER, *Finite time Lyapunov exponent and advection-diffusion equation*, Phys. D, 95 (1996), pp. 283–305, https://doi.org/10.1016/0167-2789(96)00064-4.

[34] J.-L. THIFFEAULT, *Advection-diffusion in Lagrangian coordinates*, Phys. Lett. A, 309 (2003), pp. 415–422, https://doi.org/10.1016/S0375-9601(03)00244-5.

[35] M. TODA, T. KOMATSUZAKI, T. KONISHI, R. S. BERRY, AND S. A. RICE, EDS., *Geometrical Structures of Phase Space in Multi-dimensional Chaos: Applications to Chemical Reaction Dynamics in Complex Systems*, Adv. Chemical Physics 130, John Wiley & Sons, New York, 2005.

[36] J. B. WEISS AND A. PROVENZALE, EDS., *Transport and Mixing in Geophysical Flows: Creators of Modern Physics*, Lecture Notes in Phys. 744, Springer, Berlin, 2008, https://doi.org/10.1007/978-3-540-75215-8.

[37] Y. ZHONG, A. BRACCO, AND T. A. VILLAREAL, *Pattern formation at the ocean surface: Sargassum distribution and the role of the eddy field*, Limnology Oceanography Fluids Environments, 2 (2012), pp. 12–27, https://doi.org/10.1215/21573689-1573372.